

1           **Multivariate patterns between brain network properties,**  
2           **polygenic scores, phenotypes, and environment in**  
3           **preadolescents**

4  
5 Jungwoo Seo<sup>1</sup>, Eunji Lee<sup>2</sup>, Bo-gyeom Kim<sup>2</sup>, Gakyung Kim<sup>1</sup>, Yoonjung Yoonie Joo<sup>3</sup>,  
6 Jiook Cha<sup>1, 2, 4, 5</sup>

7       1. Department of Brain and Cognitive Sciences, College of Natural Sciences,  
8       Seoul National University, Seoul, South Korea

9       2. Department of Psychology, College of Social Sciences, Seoul National  
10      University, Seoul, South Korea

11     3. Institute of Data Science, Korea University, Seoul, South Korea

12     4. Institute of Psychological Science, Seoul National University, Seoul, South  
13     Korea

14     5. Graduate School of Artificial Intelligence, Seoul National University, Seoul,  
15     South Korea

16  
17 **Correspondence to:**

18 Jiook Cha, PhD

19       Gwanak-ro 1, Building 16, Suite M512, Gwanakgu, Seoul, 08826, South  
20       Korea, [connectome@snu.ac.kr](mailto:connectome@snu.ac.kr)

## 22 **Abstract**

23 The brain network is an infrastructure for cognitive and behavioral processes.  
24 Genetic and environmental factors influence the development of the brain network.  
25 However, little is known about how specific genetic traits and children's brain network  
26 properties are related. Furthermore, insight into the holistic relationship of brain  
27 network properties with genes, environment, and phenotypic outcomes in children is  
28 still limited. To fill these knowledge gaps, we investigated the multivariate  
29 associations between the brain network properties and three domains using a large  
30 youth sample (the ABCD study, N=9,393, 9-10 years old): (i) genetic predisposition  
31 of various traits, (ii) phenotypic outcomes, and (iii) environmental factors. We  
32 constructed structural brain networks using probabilistic tractography and estimated  
33 nodal and global network measures such as degree and network efficiency. We then  
34 conducted sparse canonical correlation analysis with brain network measures and  
35 polygenic scores of 30 complex traits (e.g., IQ), phenotypic traits (e.g., cognitive  
36 ability), and environmental variables. We found multivariate associations of brain  
37 network properties with (i) genetic risk for psychiatric disorders, (ii) genetic influence  
38 on cognitive ability, and (iii) the phenotype of cognitive ability-psychopathology in  
39 preadolescents. Our subsequent mediation analysis using the latent variables from  
40 the canonical correlation analysis showed that the influence of genetic factors for  
41 cognitive ability on the cognitive outcomes was partially mediated by the brain  
42 network properties. Taken together, this study shows the key role of the development  
43 of the brain structural network in children in cognitive development with its tight, likely  
44 causal, relationship with genetic factors. These findings may shed light on future

- 45 studies of the longitudinal deviations of those gene-environment-brain network
- 46 relationships in normal and disease conditions.

## 47 Introduction

48 Childhood and adolescence are critical periods for brain development  
49 (Bethlehem et al., 2022). Proper brain development during this time is vital for  
50 cognitive and behavioral maturation (Bunge & Wright, 2007; Luna et al., 2010) and  
51 mental health (Fornito et al., 2015; Paus et al., 2008). Such development is influenced  
52 by genetic and environmental factors. Therefore, understanding the connections  
53 between the brain, cognitive-behavioral traits in children, and the impact of genetics  
54 and the environment on brain development is crucial in developmental and clinical  
55 neuroscience. The Adolescent Brain and Cognitive Development (ABCD) study  
56 (Jernigan et al., 2018) provides a rich dataset, encompassing genetic, neuroimaging,  
57 environmental, and phenotypic data for over 10,000 children aged 9-10 years old at  
58 baseline. This dataset opens an unprecedented opportunity to explore the connections  
59 between genes, environment, brain, and phenotypic outcomes more robustly with less  
60 concern about sampling bias (Marek et al., 2022) and age-confounding effects.

61 The brain is a complex network of tissues that communicate through white  
62 matter bundles. Diffusion MRI and tractography enable the reconstruction of the  
63 structural brain network (Jeurissen et al., 2019; Sotiropoulos & Zalesky, 2019). Graph  
64 theory (Rubinov & Sporns, 2010) allows us to estimate the brain network properties  
65 embedded in the whole brain's complex connectivity. The heritability of the brain  
66 network properties in youth ranges from 25% to 70% (Koenis et al., 2015; van den  
67 Heuvel, van Soelen, et al., 2013), indicating a strong genetic influence on shaping  
68 brain networks. However, little is known about which specific genetic traits and  
69 children's brain network properties are related. The recent development of the  
70 polygenic score approach (Torkamani et al., 2018) has paved the way to quantify the

71 genetic propensity of specific traits, such as bipolar disorder, and explore which  
72 genetic predispositions are related to the brain network properties.

73 Brain network properties are associated with cognitive abilities (Bathelt et al.,  
74 2018; Kim et al., 2016; Koenis et al., 2015; Ma et al., 2017; Suprano et al., 2020),  
75 psychiatric disorders (Alexander-Bloch et al., 2010; Collin et al., 2017; Rudie et al.,  
76 2012), and environmental factors such as socioeconomic status (D. J. Kim et al., 2019;  
77 Tooley et al., 2020) throughout the developmental period. Despite valuable insights  
78 from previous studies, a comprehensive understanding of the holistic relationship of  
79 brain network properties with genes, environment, and phenotypic outcomes in  
80 children is still limited due to the predominant use of univariate approaches. No single  
81 measurement is enough to characterize complex genes, brain networks, environment,  
82 and phenotypes information. Rather, combining a range of variables can capture  
83 complex traits more appropriately. Multivariate analysis, such as canonical correlation  
84 analysis (CCA), is useful for investigating holistic relationships underlying a set of  
85 variables simultaneously. CCA reveals multivariate associations linking sets of  
86 variables from two domains by maximizing the canonical correlation between them  
87 (Hotelling, 1936; Wang et al., 2020). For this reason, CCA has been extensively  
88 employed in studying links between the brain, cognition, genes, and environment  
89 (Alnaes et al., 2020; Fernandez-Cabello et al., 2022; Modabbernia et al., 2021; Smith  
90 et al., 2015; Wang et al., 2020).

91 This study aims to investigate the multivariate associations between structural  
92 brain network properties and three different domains in preadolescents: (i) genetic  
93 predisposition of various traits, (ii) phenotypic outcomes, and (iii) environmental factors.  
94 To achieve this, we leveraged the largest available childhood dataset (i.e., ABCD study)

95 and analysis techniques such as the polygenic score approach and sparse canonical  
96 correlation analysis (Witten et al., 2009).

97

## 98 **Materials and Methods**

### 99 **ABCD participants**

100 We used genetic, neuroimaging, environmental, and phenotypic data from  
101 the Adolescent Brain Cognitive Development (ABCD) study release 2.0 and 3.0  
102 (<http://abcdstudy.org>). The ABCD study, which is the largest longitudinal investigation  
103 of brain development and child health in the United States, recruited multiethnic  
104 children (N=11,875) aged 9-10 years from 21 research sites with self-reported  
105 ethnicities that comprised of 52.3% Caucasians, 20.3% Mexican Americans, 14.7%  
106 African Americans, and 12.5% Asian-Americans and others. All participants and their  
107 parents or legal guardians provided informed consent and assent forms before  
108 participating in the study.

109

### 110 **Genotype Data**

111 The saliva DNA samples of study participants were collected, and 733,293  
112 single nucleotide polymorphisms (SNPs) were genotyped at Rutgers University Cell  
113 and DNA Repository (RUCDR) with Affymetrix NIDA Smoke Screen Array. We  
114 excluded SNPs with genotype call rate <95%, sample call rate <95%, and minor  
115 allele frequency (MAF) <1%. The genotypes were imputed using the Michigan  
116 Imputation Server (Das et al., 2016) using the 1000 Genome phase3 version5 panel  
117 (Genomes Project et al., 2015) with Eagle v2.4 phasing (Loh et al., 2016). Then, the  
118 imputed variants with INFO score > .3 that did not meet our quality control criteria  
119 (i.e., call rate <95%, MAF <1%, and Hardy–Weinberg equilibrium p-value <1e-6)

120 were additionally filtered out. To address potential bias derived from genetically  
121 diverse and related family members in the ABCD study, we employed PC-Air  
122 (Conomos et al., 2015) and PC-Relate (Conomos et al., 2016) to obtain genetically  
123 unrelated individuals beyond 4th-degree relatives (i.e., kinship coefficient  $>0.022$ )  
124 and to remove outliers beyond 6 SD limits from the center of ancestrally informative  
125 principal component (PC) space. After quality control procedures, we included a total  
126 of 11,301,999 variants in 10,199 unrelated multiethnic participants, among whom  
127 7,893 participants were of European ancestry.

128

### 129 **Polygenic Scores (PGSs)**

130 We used publicly available European-based GWAS summary statistics to  
131 calculate PGSs for 30 distinct traits: Attention-deficit/hyperactivity disorder (ADHD)  
132 (Demontis et al., 2019), cognitive performance (CP) (Lee et al., 2018), educational  
133 attainment (EA) (Lee et al., 2018), major depressive disorder (MDD) (Wray et al.,  
134 2018), insomnia (Jansen et al., 2019), snoring (Jansen et al., 2019), intelligence  
135 quotient (IQ) (Savage et al., 2018), post-traumatic stress disorder (PTSD) (Nievergelt  
136 et al., 2019), depression (DEP) (Howard et al., 2019; Shen et al., 2020), body mass  
137 index (BMI) (Akiyama et al., 2017; Locke et al., 2015), alcohol dependence  
138 (ALCDEP) (Walters et al., 2018), autism spectrum disorder (ASD) (Grove et al.,  
139 2019), automobile speeding propensity (ASP) (Akiyama et al., 2017), bipolar  
140 disorder (BIP) (Stahl et al., 2019), cannabis during lifetimes (Cannabis) (Pasman et  
141 al., 2019), ever smoker (Karlsson Linner et al., 2019), shared effects on five major  
142 psychiatric disorder (CROSS) (Cross-Disorder Group of the Psychiatric Genomics,



143 2013), alcoholic drinks consumption per week (Drinking) (Karlsson Linner et al.,  
144 2019), eating disorder (ED) (Watson et al., 2019), neuroticism (Nagel et al., 2018),  
145 obsessive-compulsive disorder (OCD) (International Obsessive Compulsive Disorder  
146 Foundation Genetics & Studies, 2018), first principal components of four risky  
147 behaviors (Risky Behav) (Karlsson Linner et al., 2019), general risk tolerance  
148 (RiskTol) (Karlsson Linner et al., 2019), schizophrenia (SCZ) (Bipolar et al., 2018;  
149 Lam et al., 2019), worrying (Nagel et al., 2018), anxiety (Otowa et al., 2016),  
150 subjective well-being (SWB) (Okbay et al., 2016), general happiness (UK Biobank  
151 GWAS. Neale Lab. <http://www.nealelab.is/ukbiobank/>), and general happiness for  
152 health (happiness-health) (UK Biobank GWAS. Neale Lab.  
153 <http://www.nealelab.is/ukbiobank/>) and meaningful life (happiness-meaning) (UK  
154 Biobank GWAS. Neale Lab. <http://www.nealelab.is/ukbiobank/>).

155 The GWAS summary statistics were used as input for PRS-CS (Ge et al.,  
156 2019), a Bayesian regression method, to estimate the posterior effect sizes of SNPs.  
157 The final scores were calculated using PLINK v1.9. To optimize the scores, we  
158 followed the suggestion of the original PRS-CS paper and chose the optimal global  
159 shrinkage hyperparameter ( $\phi$ ) from among four possible values: 1, 1e-2, 1e-4,  
160 and 1e-6. The validation procedure was carried out within 14 PGSs (i.e., DEP, MDD,  
161 ADHD, general happiness, happiness-health, happiness-meaning, SWB, insomnia,  
162 snoring, BMI, PTSD, CP, EA, IQ) that had related measures in the ABCD study. For  
163 each PGS, we performed linear regression of the phenotype variable with each of  
164 the four scores and covariates (sex, age, and the first ten genetic PCs), and then,  
165 based on  $R^2$  and beta coefficient of PGS, selected one of the four PGSs. The  
166 remaining 16 PGSs was automatically validated by PRS-CS-auto (Ge et al., 2019),

167 which select the optimal value of global shrinkage parameter employing a Bayesian  
168 approach. Finally, to minimize the bias from population stratification, we residualized  
169 the final PGSs with the first ten genetic PCs.

170

## 171 **Environmental Factors**

172 To investigate the relationship between children's brain network properties  
173 and their environment, we examined 121 environmental and culture-related variables  
174 for analysis. The variables consist of 80 variables representing the family history of  
175 various problems (e.g., alcohol problem, drug use problem, depression, suicide-  
176 related problem, etc.), 19 variables related to the residential history derived area  
177 deprivation index (ADI), 11 parent characteristics and family culture related variables,  
178 and others (e.g., perinatal condition, school environment, neighborhood safety, etc.).

179 To retain the sample as much as possible, we imputed missing values. For  
180 categorical variables, we replaced the missing values with the most frequent value  
181 (mode imputation); for continuous variables, with medians. Next, variables with near  
182 zero variance were eliminated. We finally used 75 environmental variables for the  
183 statistical analysis.

184

## 185 **Phenotype Data**

186 To investigate the relationship between children's brain network properties  
187 and their mental health, physical health, and neurocognitive capacity, we examined  
188 174 phenotypic variables. These included 89 mental health and abnormal behaviors

189 related variables (e.g., KSAD diagnosis, Child Behavior Checklist), 74 physical  
190 health-related variables (e.g., physical disorders, medical history), and 10 NIH  
191 Toolbox cognitive assessment variables and a delay discounting related variable  
192 (i.e., cash choice task score). We also preprocessed the missing values with mode  
193 imputation for categorical variables and median imputation for continuous variables.  
194 Among phenotype data, variables having near zero variance were removed. We  
195 finally used 117 phenotype variables for the statistical analysis after variable  
196 selection based on the variance.

197

## 198 **Structural Brain Network Construction**

199 Detailed procedures for acquiring and preprocessing MRI data are described  
200 in (Kim et al., 2022). To estimate brain structural networks from neuroimaging,  
201 individual connectome data was generated. This was achieved by applying MRtrix3  
202 (Tournier et al., 2019) to the preprocessed dMRI data to estimate whole-brain white  
203 matter tracts and generate individualized connectomes. Probabilistic tractography  
204 was performed using constrained-spherical deconvolution (CSD) (Calamante et al.,  
205 2010; Tournier et al., 2007) with random seeding across the brain and target  
206 streamline counts of 20 million. Initial tractograms were filtered using spherical-  
207 deconvolution informed filtering (2:1 ratio)(Smith et al., 2013), resulting in a final  
208 streamline count of 10 million. An 84x84 whole-brain connectome matrix was  
209 generated for each participant using the T1-based parcellation and segmentation  
210 from FreeSurfer with Desikan-Killiany atlas (Desikan et al., 2006)(68 nodes for the  
211 cortical region and 16 nodes for the subcortical region). This approach ensured that

212 individual participants' connectomes were based on their neuroanatomy. The  
213 computation was conducted on supercomputers at Argonne Leadership Computing  
214 Facility Theta and Texas Advanced Computing Center Stampede2.

215

## 216 **Brain Network Measures (BNMs)**

217 We used the connectome matrix to construct an undirect weighted graph  
218 representing the structural brain network. Nodes and edges in the graph represent  
219 parcellated gray matter regions and connections between them, respectively.  
220 Connection strength was quantified by the streamline count. To account for the  
221 potential false positive connections generated by probabilistic tractography and their  
222 impact on network topology, we eliminated extremely weak connections (streamline  
223 counts less than 3). After thresholding, we excluded individuals with at least one  
224 isolated node, assuming all brain regions are communicable via at least one path.

225 We calculated 18 different types of brain network measurements (BNMs)  
226 representing different aspects of brain network's property (Rubinov & Sporns, 2010;  
227 van den Heuvel & Sporns, 2011). We calculated eight global graph metrics (including  
228 network density, modularity, normalized modularity, normalized average clustering  
229 coefficient, normalized characteristic path length, global efficiency, normalized global  
230 efficiency, small worldness) and five nodal graph metrics (including degree, strength,  
231 clustering coefficient, betweenness centrality, nodal efficiency) to represent brain  
232 network's global and regional properties. In addition, to examine rich club  
233 organization, we also calculated raw and normalized rich club coefficient (van den  
234 Heuvel & Sporns, 2011) of the network and the strength of rich club connection,

235 feeder connection, and local connection. Brain regions with top 12% degree were  
236 defined as rich club nodes following previous work (van den Heuvel, Sporns, et al.,  
237 2013). All graph measures were calculated using the package Brain Connectivity  
238 Toolbox (<https://sites.google.com/site/bctnet/>).

239

## 240 **Sparse Canonical Correlation Analysis**

241 To examine a latent mode of covariation between structural brain network  
242 properties and various polygenic scores, environmental factors, and phenotypic  
243 outcomes, we used sparse canonical correlation analysis (Witten et al., 2009)  
244 between brain network measures and three types of non-imaging data (i.e., PGSs,  
245 environmental variables, phenotype variables) separately. Canonical correlation  
246 analysis (CCA) is a multivariate procedure that maximizes the correlation between  
247 the linear combinations of two sets of variables. Sparse canonical correlation  
248 analysis is one of the popular variants of CCA with L1 regularization for sparse  
249 solutions. We used sparse canonical correlation analysis to avoid over-fitting and  
250 improve interpretability from sparse solutions.

251 The most popular algorithm for sparse canonical correlation analysis is  
252 penalized matrix decomposition (PMD)(Witten et al., 2009), which solves  
253 optimization problem of below equation for given two sets of data matrix  $X_{n \times p}$ ,  $Y_{n \times q}$ .  
254 (n: sample size; p, q: the number of variables of domain X and Y respectively; u, v:  
255 canonical weights of domain X and Y respectively; c1, c2: regularization parameter)

$$256 \max cov(Xu, Yv)$$

257  $s.t. \|u\|_2 = \|v\|_2 = 1, \|u\|_1 \leq c_1, \|v\|_1 \leq c_2$

258 To interpret Witten's sparse canonical correlation analysis as correlation  
259 maximization, we need to assume covariance matrices  $X^T X, Y^T Y$  are identity  
260 matrices (Witten et al., 2009). But in our study with the high dimensional brain  
261 datasets, the assumption is hardly satisfied (Fig. S1). For this reason, we interpreted  
262 Witten's sparse canonical correlation analysis as a maximizing covariance algorithm  
263 between two sets of variables rather than maximizing correlation.

264 To test generalizability of the sparse canonical correlation analysis results,  
265 we split the dataset into a training and test set. For sparse canonical correlation  
266 analysis with PGS and brain network measures, we split train set (n=5,411) and test  
267 set (n=1,145) based on genetic relatedness to avoid including biological family in the  
268 same dataset. In addition, we only used participants classified as genetically  
269 European ancestry to control genetic confounding effects for sparse canonical  
270 correlation analysis with PGSs. For sparse canonical correlation analysis with  
271 environmental factors and phenotype data, we used stratified train (80%) - test  
272 (20%) split by family history of various problems and KSAD diagnosis respectively.  
273 **Table 2** summarizes the demographic information of the samples included in this  
274 study.

275 We attempted to control the potential confounding effects by regressing out  
276 the variance explained by age, sex, parental education, household income, marital  
277 status, race ethnicity, BMI, and ABCD-site out of brain network measures,  
278 environmental factors, and phenotype data. For binary variables such as family  
279 history and KSADS-COMP, we regressed out with logistic regression. Residualized  
280 data was used for the input of sparse canonical correlation analysis. On the other

281 hand, for polygenic scores, we did not regress out from PGSs because listed  
282 covariates may not contaminate genetic information.

283 We selected optimal L1 regularization parameters from 5-fold cross validation  
284 searching from 0.1 to 1 with a step size of 0.05 for both X and Y variables  
285 respectively. The optimal L1 parameter combination was selected to maximize the  
286 covariance of validation set between canonical variates of the first component (Fig.  
287 S2).

288 For each sparse canonical correlation analysis, we extracted five modes of  
289 covariance. To examine the statistical significance of each mode, we used a  
290 permutation test. By randomly shuffling the rows of one dataset and remaining the  
291 other, we generated 5,000 permutation sets. The p-value of each component was  
292 calculated based on the number of permutation sets having greater covariance than  
293 that obtained from the original dataset, and FDR-correction was done within each  
294 CCA.

295 
$$p_{uncorrected} = \frac{N_{null\ cov > cov}}{N_{null}}$$

296

297 Selected variables and their loading depend on the input sample. To find variables  
298 reliably related to each mode, we used bootstrap resampling. We randomly  
299 resampled 5,000 times with replacement and assessed the 95% confidence interval  
300 of each variable's loading and how consistently it was selected. We interpreted the  
301 significant modes based on loading patterns of variables whose 95% confidence  
302 interval of loading does not cross zero (Xia et al., 2018) and selected more

303 frequently than expected by chance (i.e., more frequently selected than expected by  
304 binomial distribution). Because sparse canonical correlation analysis with bootstrap  
305 sample may change the order of components (axis rotation) and signs (reflection)  
306 (Misic et al., 2016; Xia et al., 2018), the re-alignment procedure is needed to  
307 estimate confidence interval of loading properly. We matched the components and  
308 signs based on cosine similarity of weight vectors obtained from original dataset and  
309 bootstrap sample. To assess the reproducibility of the findings, we applied the model  
310 to the held-out test set and estimated significance of each mode through the  
311 permutation test.

312

## 313 **Mediation Analysis**

314 After sparse canonical correlation analysis, we raised a hypothesis that the  
315 genetic factors of cognitive ability may influence the phenotype of cognitive ability-  
316 psychopathology through brain network properties (Results – Mediation Analysis). To  
317 test the hypothesis, we examined whether brain network property scores related to  
318 the genetic predisposition of cognitive ability (i.e., BNM score of PGS-BNM mode 2)  
319 mediated the relationship between polygenic scores for cognitive ability (i.e., PGS  
320 score of PGS-BNM mode 2) and the phenotype of cognitive ability-psychopathology  
321 (i.e., phenotype score of Phenotype-BNM mode 2). Age, sex, race ethnicity, parental  
322 education, household income, marital status, ABCD site, and BMI were used as  
323 covariates in the mediation analysis. The two-sided p-values for each path were  
324 estimated from 500 bootstrap samples.



## 325 Results

### 326 Modes of covariation between polygenic scores and structural brain network 327 properties

328 Using sparse canonical correlation analysis, we investigated the relationship  
329 between 30 genome-wide polygenic scores (PGSs) and measures of brain network  
330 properties (BNMs). Our analysis revealed a significant mode (mode 1) and a mode  
331 that showed marginal significance (mode 2) (mode 1:  $p = 0.006$  ,  $cov = 0.846$  ,  $r =$   
332  $0.107$  ; mode 2:  $p = 0.0545$  ( $p_{unc} = 0.021$ ),  $cov = 0.585$  ,  $r = 0.118$  , all p-values  
333 were FDR corrected). Detailed results of the permutation test and the loading patterns  
334 for all five modes can be found in the supplementary material (Fig. S3, S4).

335 The first mode of PGSs showed significant positive loadings for PGSs related  
336 to psychiatric disorders, such as bipolar disorder and cross disorder (**Fig. 1a**). On the  
337 brain side, normalized clustering and rich club coefficients showed positive loadings,  
338 while network density, degree, and raw rich club coefficients, and the connection  
339 strengths (among the bilateral rostral anterior cingulate, rostral middle frontal,  
340 paracentral, lingual regions, and cerebellums) showed negative loadings (**Fig. 1b**,  
341 **S4**).

342 In the second mode of the PGSs, we observed strong positive loadings for  
343 PGSs related to cognitive abilities, such as cognitive performance (CP) and IQ.  
344 Meanwhile, there were weak negative loadings for material use-related PGSs (**Fig.**  
345 **1c**). In terms of corresponding brain network properties, positive loadings were found  
346 for connection strength, betweenness centrality, normalized nodal efficiency of  
347 middle temporal gyrus, and betweenness centrality of the left inferior parietal area.

348 On the other hand, the strength of posterior cingulate cortex, thalamus, and caudate,  
349 as well as feeder and rich club connection strength had negative loadings (**Fig. 1d,**  
350 **S4**). To sum up, the polygenic scores for higher cognitive ability were positively  
351 linked to network integrity of the middle temporal gyrus and negatively associated  
352 with connection strength of the posterior cingulate cortex, thalamus, and caudate.

353

### 354 **Modes of covariation between phenotypes and structural brain network** 355 **properties**

356 Among the five modes of covariation, only the second and the third mode were  
357 significant and generalized to the hold-out test sets (mode 2:  $p < 0.001$ ,  $cov = 1.069$ ,  
358  $r = 0.119$ ; mode 3:  $p = 0.016$ ,  $cov = 0.640$ ,  $r = 0.089$ , all  $p$ -values were FDR corrected).  
359 We thus interpreted the second and third modes only. Detailed results of the  
360 permutation test and the loading patterns for all five modes can be found in the  
361 supplementary material (Fig. S5, S6).

362 The second mode of phenotypes depicted the covariation between brain  
363 network properties and the shared characteristics of cognitive ability and  
364 psychopathology (cognitive ability-psychopathology) (**Fig. 1e, 1f, S6**). Cognitive test  
365 scores (i.e., NIH Toolbox scores) showed positive loadings, whereas  
366 psychopathologic traits, such as CBCL and PGBI mania scores, showed negative  
367 loadings. Several brain network properties showed loading patterns similar to that of  
368 polygenic scores for cognitive ability (i.e., PGS mode 2). Consistent with the loadings  
369 observed in PGS mode 2, the connection strength and nodal efficiency of the middle  
370 temporal gyrus and betweenness centrality of the left inferior parietal region showed

371 positive loadings, while the strength of the posterior cingulate cortex, thalamus, and  
372 caudate, along with the feeder and rich club connections, showed negative loadings.  
373 Conversely, certain network properties were found to be statistically significant only  
374 in relation to phenotypes. The nodal efficiency of the superior temporal region and  
375 the betweenness centrality of the postcentral and supramarginal regions showed  
376 positive loadings. Additionally, the strength of the anterior cingulate, paracentral, and  
377 overall subcortical regions, as well as the nodal efficiency of the insula and  
378 hippocampus, showed negative loadings. To summarize, phenotypes of cognitive  
379 ability-psychopathology were positively associated with the network integrity of the  
380 temporal and inferior parietal cortex, while being negatively associated with the  
381 connection strength of the cingulate and subcortical regions.

382           Despite strong negative loadings in the NIH Toolbox scores, the third mode  
383 did not show any significant features (Fig. S6).

384

### 385 **Modes of covariation between environmental factors and structural brain** 386 **network properties**

387           Among the five modes analyzed, the second mode showed a marginal level  
388 of statistical significance, while the third mode showed a significant relationship  
389 (mode 2:  $p = 0.092$  ( $p_{unc} = 0.0402$ ),  $cov = 0.896$ ,  $r = 0.074$  ; mode 3:  $p = 0.016$ ,  
390  $cov = 0.802$ ,  $r = 0.124$ , all p-values were FDR corrected). Further information  
391 regarding the results of the permutation test and the loading patterns for all five  
392 modes can be found in the supplementary material (Fig. S7, S8).

393           The second mode showed the relationship between environmental factors  
394 related to socioeconomic status and brain network properties. Variables representing  
395 socioeconomic advantages showed positive loadings, whereas variables  
396 representing socioeconomic disadvantages showed negative loadings (**Fig. 2**).  
397 Regarding its relationship with brain network properties, only the nodal efficiency of  
398 the right hippocampus showed a significant association with the second mode (**Table**  
399 **4**).

400           The third mode depicted the relationship between perinatal conditions, such  
401 as caesarian section and age of parents, and brain network properties (**Fig. 2**).  
402 Perinatal conditions showed positive associations with certain brain network  
403 properties (**Table. 4**). Specifically, the connection strength, betweenness centrality,  
404 and clustering coefficient of the entorhinal cortex showed positive loadings. In  
405 contrast, the strength of the precentral gyrus, cerebellum, and thalamus, as well as  
406 the nodal efficiency of the cerebellum and the degree of the caudate, showed  
407 negative loadings.

408

## 409 **Mediation Analysis**

410           We discovered that both polygenic scores and phenotypes related to  
411 cognitive ability shared covarying brain network properties. Specifically, we observed  
412 shared brain network properties, including the connection strength and nodal  
413 efficiency of the middle temporal gyrus, betweenness centrality of inferior parietal  
414 regions, and the connection strength of the posterior cingulate cortex and thalamus  
415 (**Fig. 1d, 1f**). These findings led us to the hypothesis that the genetic factors

416 influencing cognitive ability may exert their influence through brain network  
417 properties.

418 To test this hypothesis, we examined whether the BNM score of PGS-BNM  
419 mode 2 serves as a mediator between the PGS score of PGS-BNM mode 2 and the  
420 phenotype score of phenotype-BNM mode 2 (**Fig. 3**). The result demonstrated that  
421 brain network properties significantly mediated the relationship between polygenic  
422 scores for cognitive ability and the phenotype of cognitive ability-psychopathology  
423 (indirect effect = 0.013,  $p < 0.001$ ).

## 424 Discussion

425 This study investigated the multivariate relationship of brain network  
426 properties with genes, environment, and phenotypic outcomes in children. We  
427 discovered multiple modes of covariation among the structural brain network  
428 properties and the following factors: (i) the genetic propensity for psychiatric  
429 disorders and cognitive capacity, (ii) the phenotypic outcomes related to the cognitive  
430 ability and psychopathology, and (iii) the environmental factors, such as  
431 socioeconomic status and perinatal conditions. Additionally, our study showed that  
432 the brain network mediates the effects of the polygenic scores for cognitive capacity  
433 on phenotypic outcomes of cognitive ability and psychopathology. This study offers  
434 insight into which genetic factors are related to the brain network properties and the  
435 multivariate relationships among variables of brain network properties, genes,  
436 environmental factors, and phenotypic outcomes in children. It gives rise to  
437 discussions about the underlying biology of brain network and cognitive development  
438 and further hypotheses in this field.

439 In the sparse canonical correlation analysis with phenotypes, we observed  
440 that the cognitive intelligence (NIH Toolbox) and psychopathology phenotypes  
441 (CBCL) exhibited a single mode of covariation rather than distinct modes. This single  
442 mode suggests that children's cognitive ability and abnormal behavior share  
443 underlying brain network properties but with opposite signs of correlations. This  
444 finding resembles previous findings, for instance, a single mode of positive-negative  
445 behavioral and genetic traits covarying with brain connectivity (Smith et al., 2015;  
446 Taquet et al., 2021).

447 Our mediation analysis showed that the brain network mediated genetic  
448 predisposition and phenotypic outcomes of cognition and psychopathology during  
449 childhood. This mediation may be facilitated by specific brain network properties  
450 associated with both the polygenic scores for cognitive abilities and phenotypes  
451 related to cognitive ability-psychopathology. Further investigation is necessary to  
452 determine the extent of the involvement of these common network properties in the  
453 gene-brain network-phenotypic outcome pathway. Mediation through the brain  
454 network properties accounts for approximately 5% of the gene-phenotype pathway of  
455 intelligence, implying other pathways, such as through cortical surface area or  
456 thickness (Lett et al., 2020).

457 Children with higher polygenic scores for cognitive abilities or phenotype  
458 scores of cognitive ability-psychopathology showed greater nodal efficiency in the  
459 middle temporal gyrus and inferior parietal region. These regions are constituents of  
460 the system proposed by the parieto-frontal integration theory (P-FIT) of intelligence  
461 (Jung & Haier, 2007) and play a crucial role in semantic, language, and number  
462 processing (Binder et al., 2009; Seghier, 2013; Visser et al., 2012). In contrast,  
463 children with lower scores on cognitive ability-psychopathology exhibited greater  
464 nodal efficiency in the hippocampus and insula. These regions have been implicated  
465 in various cognitive functions, including learning, memory, emotional regulation, and  
466 interoception (Jarrard, 1993; Namkung et al., 2017; Phelps, 2004; Rubin et al., 2014;  
467 Sweatt, 2004). While previous studies have reported a positive correlation between  
468 global efficiency and children's intelligence (Bathelt et al., 2018; Kim et al., 2016; Ma  
469 et al., 2017), our results did not. Our study suggests that the relationship between  
470 intelligence and network efficiency is more closely linked to the network efficiency of

471 some brain regions, such as the temporal and parietal regions, rather than the  
472 overall global efficiency.

473 Our results indicate a negative association between the connection strength  
474 of the posterior cingulate cortex and subcortical regions and polygenic scores and  
475 phenotypes related to cognitive ability. During childhood and adolescence, FA of  
476 white matter is known to increase (Tamnes et al., 2018). Unlike studies based on FA,  
477 research has reported decreased streamline counts and density during this period,  
478 particularly in connections with higher streamline counts and those linked to  
479 subcortical regions (Baker et al., 2015; Lim et al., 2015). Considering these  
480 documented changes in white matter connectivity, the observed negative association  
481 may indicate a progression in white matter development among children with higher  
482 cognitive abilities.

483 Our study suggests that children with higher polygenic scores for psychiatric  
484 disorders have lower network density and degree across various brain regions.  
485 Individuals with psychiatric disorders are known to have less white matter connection  
486 (Chen et al., 2021; Perry et al., 2019; van den Heuvel & Fornito, 2014). These  
487 findings suggest that the tendency of less white matter connections in individuals  
488 with a higher genetic risk for psychiatric disorders is already observable in 9-10  
489 years old. It is aligned with the findings that youth with higher genetic risks for  
490 psychiatric disorders have smaller white matter volume and average connection  
491 strength (Fernandez-Cabello et al., 2022; Taquet et al., 2021).

492 The wiring and maintenance of white matter tracts require significant  
493 metabolic support. For this reason, the metabolic budget of the brain is a critical



494 factor in shaping the brain network (Bullmore & Sporns, 2012). Taking into account  
495 network density is often used as a proxy for the wiring cost (Achard & Bullmore,  
496 2007; Bassett et al., 2009), lower density observed in children with higher genetic  
497 risks for psychiatric disorders may imply a link between genetic susceptibility to  
498 psychiatric disorders and abnormal brain metabolism, subsequently affecting the  
499 development of structural brain networks. Indeed, mitochondrial dysfunction has  
500 consistently been proposed as a pathological foundation of psychiatric disorders  
501 (Clay et al., 2011; Y. Kim et al., 2019; Rezin et al., 2009; Shao et al., 2008; Zuccoli et  
502 al., 2017), and recent studies identified genetic overlaps between psychiatric  
503 disorders and metabolic syndromes (Amare et al., 2017; Rodevand et al., 2021).

504         The brain network favors short-range connections over long-distance ones to  
505 minimize wiring costs, promoting local segregation within the network (Bullmore &  
506 Sporns, 2012). We observed a higher clustering coefficient in children with a higher  
507 genetic risk for psychiatric disorders, which may be related to lower brain metabolic  
508 support. Our results showed that genetic risks for psychiatric disorders were  
509 negatively associated with raw rich club coefficients at  $k=20-50$ , but positively  
510 associated with normalized rich club coefficients. Network density may partially  
511 influence these correlations (van Wijk et al., 2010).

512         Our study indicates that environmental factors, such as socioeconomic status  
513 and perinatal conditions, can affect brain network properties in children beyond mere  
514 brain morphology (Alnaes et al., 2020). Specifically, we observed a positive  
515 correlation between socioeconomic advantage and the nodal efficiency of the right  
516 hippocampus. This finding aligns with previous studies showing the impact of  
517 socioeconomic disadvantage on various aspects of the hippocampus, including gray

518 matter volume (Hanson et al., 2011; Jednorog et al., 2012), connectivity (Barch et  
519 al., 2016), and network efficiency (D. J. Kim et al., 2019). However, the significant  
520 associations between network properties and environmental factors were fewer in  
521 number compared to genetic factors. This suggests that the influence of  
522 environmental factors on brain network properties may be either less pronounced or  
523 more heterogeneous than genetic factors.

524         This study has several limitations. Firstly, we used cross-sectional data,  
525 which limits our ability to investigate the relationships between brain network  
526 properties, genes, phenotypes, and the environment over time. Although our findings  
527 provide insights into normative brain network development, a longitudinal study  
528 design is necessary to fully understand developmental trajectories. Second,  
529 polygenic scores only consider common genetic variants that reach a certain level of  
530 statistical significance in a genome-wide association study (GWAS). Thus, polygenic  
531 scores in this study do not capture the impact of rare variants or complex interactions  
532 like gene-gene and gene-environment interactions. Lastly, our statistical models only  
533 capture homogeneous linear relationships, which may not be adequate for  
534 comprehending the complex interactions (Greene et al., 2022) that occur among  
535 genetic profiles, environmental factors, phenotypic traits, and data-collection artifacts  
536 within a large population study. The small effect sizes observed in the relationship  
537 between brain network properties and genetic, phenotypic, and environmental  
538 factors ( $r = 0.074-0.124$ ) may indicate heterogeneous associations depending on  
539 covariate profiles. To gain more informative insights into the relationships among  
540 genes, environment, brain, and phenotypes, a more sophisticated model that can  
541 capture heterogeneous associations based on covariates may be necessary. For

542 instance, employing conditional (or local) average treatment effect analysis with  
543 causal machine learning (Athey et al., 2019) would be beneficial, as it would aid in  
544 personal, clinical, and political decision-making.

545

## 546 **Data Availability**

547 All original data are publicly available from the NDA  
548 (<https://nda.nih.gov/abcd/>). Mook data, which corresponds to the processed data  
549 used in this study, was generated from conditional GAN for tabular data (Xu et al.,  
550 2019) and are available from this site ([https://github.com/Transconnectome/ABCD-](https://github.com/Transconnectome/ABCD-brain-network-SCCA)  
551 [brain-network-SCCA](https://github.com/Transconnectome/ABCD-brain-network-SCCA)).

## 552 **Code Availability**

553 Code is available from here: [https://github.com/Transconnectome/ABCD-](https://github.com/Transconnectome/ABCD-brain-network-SCCA)  
554 [brain-network-SCCA](https://github.com/Transconnectome/ABCD-brain-network-SCCA).

## 555 **Funding**

556 This work was supported by the National Research Foundation of Korea  
557 (NRF) grant funded by the Korea government (MSIT) (No. 2021R1C1C1006503,  
558 2021K2A9A1A01102014, 2021K1A3A1A21037512, 2021M3E5D2A01022515), by  
559 Seoul National University Research Grant in 2021 (No. 200-20210083), by Creative-  
560 Pioneering Researchers Program through Seoul National University (No. 200-  
561 20220046), by Semi-Supervised Learning Research Grant by SAMSUNG  
562 (No.A0426-20220118), by Institute of Information & communications Technology

563 Planning & Evaluation (IITP) grant funded by the Korea government(MSIT)  
564 [NO.2021-0-01343, Artificial Intelligence Graduate School Program (Seoul National  
565 University)], and by Identify the network of brain preparation steps for concentration  
566 Research Grant by Looxid Labs (No.339-20230001).

567

## 568 **Author contributions**

- 569 ● Jungwoo Seo, Conceptualization, Data curation, Formal analysis, Validation,  
570 Investigation, Visualization, Writing – original draft, Writing – review and editing
- 571 ● Eunji Lee, Data curation, Writing – original draft, Writing – review and editing
- 572 ● Bogyom Kim, Data curation, Writing – review and editing
- 573 ● Gakyung Kim, Data curation, Writing – original draft, Writing – review and editing
- 574 ● Yoonjung Yoonie Joo, Data curation, Writing – review and editing
- 575 ● Jiook Cha, Conceptualization, Supervision, Project administration, Funding  
576 acquisition, Resources, Data curation, Writing – original draft, Writing – review and  
577 editing.

## 578 **Ethics**

## 579 **Competing Interest Disclosures**

580 None of the authors have significant competing financial, professional, or personal  
581 interests that might have influenced the performance or presentation of the work  
582 described in the manuscript.

583

584

585 **Tables**

586 **Table 1. Abbreviation of PGSs and their meaning.**

<b>Abbreviation</b>	<b>Meaning</b>
<b>CROSS</b>	Cross disorder between ASD, ADHD, bipolar disorder, MDD, and schizophrenia
<b>Neuroticism</b>	Neuroticism
<b>Risky Behav</b>	The first principal component of the four risky behaviors
<b>RiskTol</b>	General risk tolerance
<b>Worry</b>	Worrying subtype
<b>ASP</b>	Automobile speeding propensity: the tendency to drive faster than the speed limit
<b>ALCDEP</b>	Alcohol dependence
<b>ED</b>	Eating Disorder (Anorexia nervosa)
<b>Drinking</b>	Drinks per week – the average number of alcoholic drinks consumed per week
<b>ASD</b>	Autism Spectrum Disorder
<b>BIP</b>	Bipolar disorder
<b>Cannabis</b>	Cannabis during their lifetime (self-reported)
<b>Smoke</b>	Ever smoker – whether one has ever been a smoker
<b>SCZ</b>	Schizophrenia
<b>OCD</b>	Obsessive-Compulsive Disorder

<b>Anxiety</b>	Anxiety
<b>DEP</b>	Depression
<b>MDD</b>	Major Depression Disorder
<b>GHapi</b>	General Happiness
<b>GHapiHealth</b>	General Happiness - health
<b>GHapiMean</b>	General Happiness - meaningful life
<b>SWB</b>	Subjective Well Being
<b>INSOMNIA</b>	Insomnia
<b>SNORING</b>	Snoring
<b>BMI</b>	Body Mass Index
<b>PTSD</b>	Post-Traumatic Stress Disorder
<b>CP</b>	Cognitive Performance
<b>EA</b>	Education Attainment
<b>IQ</b>	Intelligence Quotient
<b>ADHD</b>	Attention-Deficit/Hyperactivity Disorder

587

588

589

**Table 2. Demographic information of the study participants.**

		PGS – BNM (n=6,549)		ENV – BNM (n=9,393)		Pheno – BNM (n=8,895)	
		train	test	train	test	train	test
N	total	5,406	1,143	7,514	1,879	7,116	1,779
Sex	Male	2,869	600	3,931	965	3,741	905
	Female	2,537	543	3,583	914	3,375	874
Race	White	3,831	865	4,167	1,041	4,086	1015
	Black	34	7	995	234	866	221
	Hispanic	993	154	1,406	401	1,269	323
	Asian	6	1	147	32	143	29
	Other	542	116	799	171	752	191

590



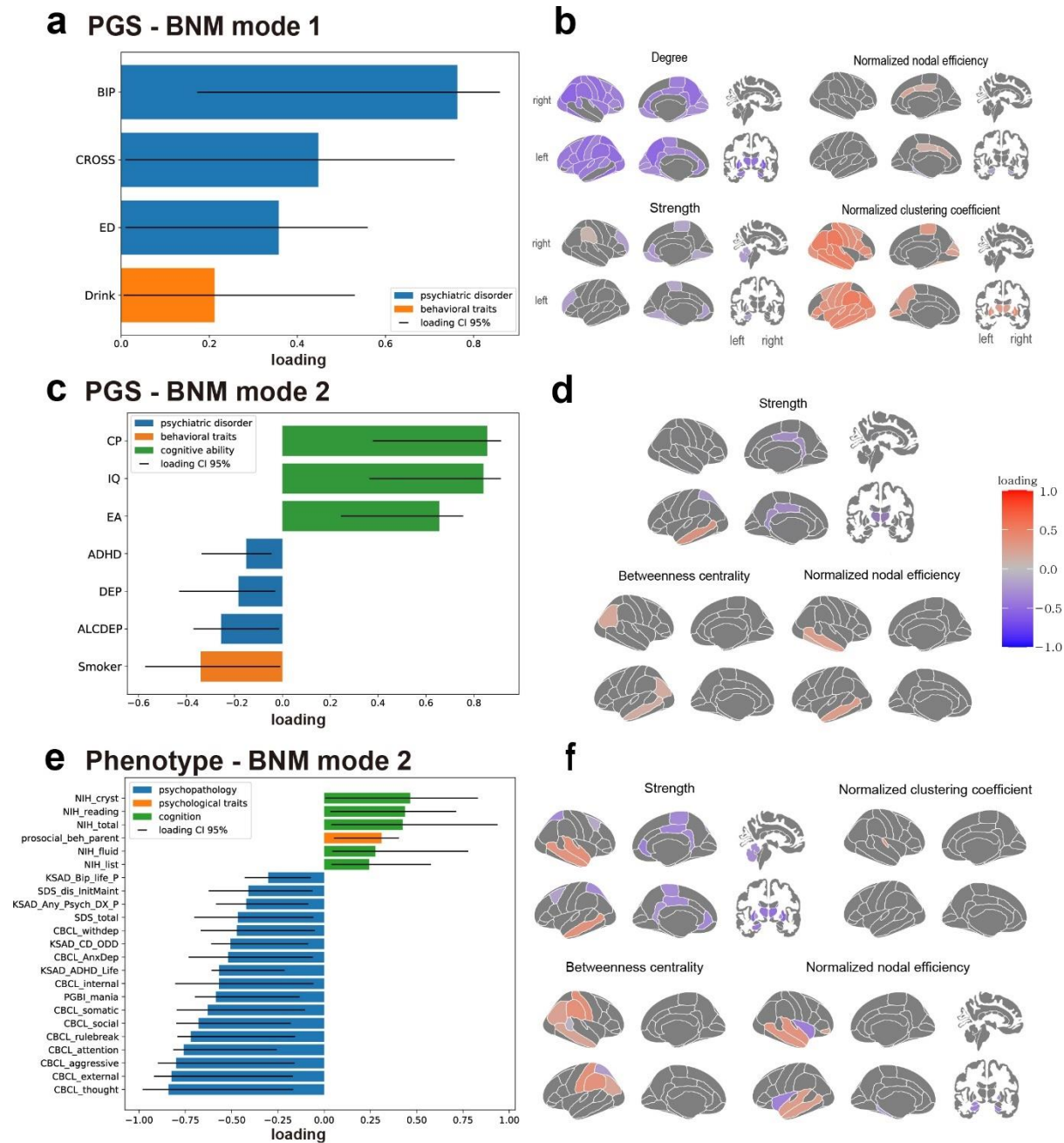
591 **Table 3. p-value, correlation coefficient, covariance of sparse**  
 592 **canonical correlation analysis results.** p-value of each mode is estimated by  
 593 permutation test. \* p\_FDR < 0.05, \*\* p\_FDR < 0.01, \*\*\* p\_FDR < 0.001, † p\_uncorrected < 0.05.

Sparse Canonical Correlation Analysis with Brain Network Metrics		Mode1	Mode2	Mode3	Mode4	Mode5
<b>Polygenic Scores</b>	p_training	<b>0.0060**</b>	0.0545 (0.0218)†	0.6633	0.9640	0.3033
	p_test	<b>0.0060**</b>	<b>0.0210*</b>	0.4582	0.1587	0.4582
	corr	<b>0.1071</b>	<b>0.1176</b>	0.1231	0.0831	0.1404
	cov	<b>0.8458</b>	<b>0.5845</b>	0.4425	0.3517	0.3830
<b>Phenotypes</b>	p_training	<b>0.0020*</b>	<b>&lt;0.001***</b>	<b>0.0160*</b>	0.2128	0.0678
	p_test	0.1020	<b>0.0060**</b>	<b>0.0110*</b>	0.1990	0.5814
	corr	0.1124	<b>0.1194</b>	<b>0.0885</b>	0.0924	0.1233
	cov	1.2243	<b>1.0692</b>	<b>0.6401</b>	0.4819	0.4593
<b>Environmental Factors</b>	p_training	0.0920	0.0920 (0.0402)†	<b>0.0160*</b>	0.5582	0.0920
	p_test	0.1227	<b>0.0145*</b>	<b>0.0030**</b>	0.4682	0.3663
	corr	0.0745	<b>0.0741</b>	<b>0.1239</b>	0.0843	0.1060
	cov	1.1196	<b>0.8956</b>	<b>0.8023</b>	0.5263	0.5226

595 **Table 4. Sparse canonical correlation analysis results of**  
 596 **environmental factors-brain network measures.** Only significant brain network  
 597 measures are presented. The loadings of corresponding environmental factors are visualized in  
 598 Figure 2.

	Region	Network measure	Loading	Loading 95% CI
<b>Mode 2</b>	Hippocampus	Nodal efficiency R-HI	0.2098	[0.0031, 0.4603]
<b>Mode 3</b>	Caudate	Deg L-CA	-0.3778	[-0.4016, -0.0038]
		Deg R-CA	-0.3753	[-0.3930, -0.0156]
	Entorhinal cortex	Stren L-EC	0.3417	[0.0336, 0.4331]
		Stren R-EC	0.3483	[0.0378, 0.4348]
		BC_L-EC	0.1091	[0.0174, 0.1560]
		Norm_clust_coef L-EC	0.3691	[0.0208, 0.4188]
		Norm_clust_coef R-EC	0.3879	[0.0357, 0.4383]
	Precentral gyrus	Stren L-PrCG	-0.4642	[-0.4978, -0.0116]
		Stren R-PrCG	-0.4356	[-0.4866, -0.0100]
	Cerebellum	Stren L-CER	-0.2761	[-0.3509, -0.0222]
		Stren R-CER	-0.2768	[-0.3465, -0.0171]
		Nodal efficiency L-CER	-0.3695	[-0.4661, -0.0615]
		Nodal efficiency R-CER	-0.3699	[-0.4646, -0.0603]
	Thalamus	Stren L-TH	-0.4175	[-0.5760, -0.0779]
Stren R-TH		-0.4141	[-0.5797, -0.0651]	

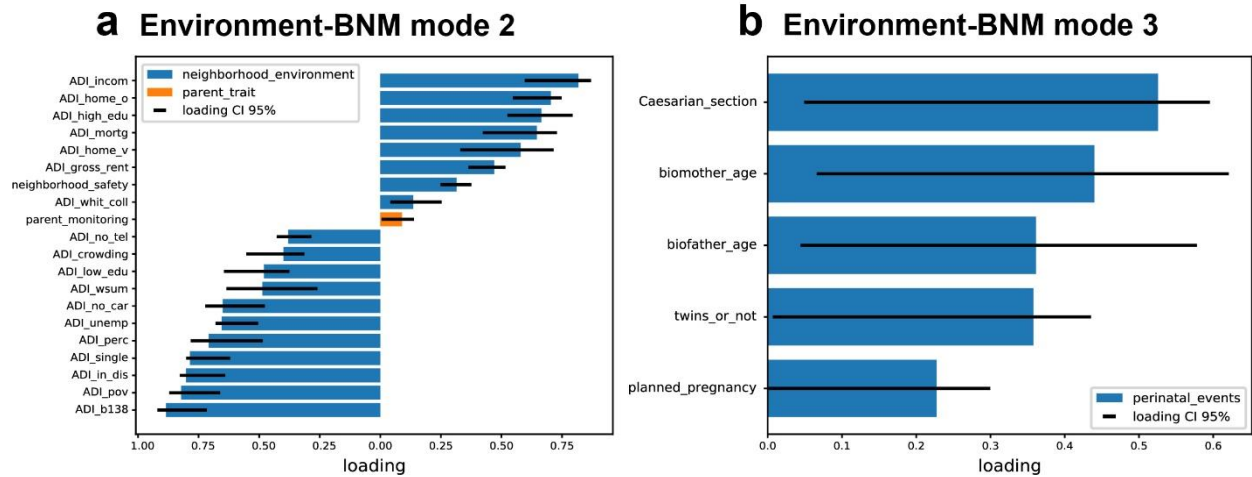
	Temporal pole	Stren R-TP	0.1590	[0.0255, 0.2223]
		Norm_clust_coef L-TP	0.3942	[0.0216, 0.4324]



600

601 **Figure 1 Sparse canonical correlation analysis results of polygenic scores-brain network**  
 602 **measures and phenotypes-brain network measures.** The results of the first and second modes of  
 603 polygenic scores (PGSs) - brain network measures (BNMs) and the second mode of phenotypes -  
 604 brain network measures. (a) The loadings of significant PGS variables in the PGSs-BNMs mode 1.  
 605 The error bars represent the 95% confidence interval of the loading, estimated from the 5,000  
 606 bootstrap samples. Among the 30 PGSs, only significant PGS variables are presented, while the  
 607 others can be found in supplementary figure 4. The color of each bar represents the category to which

608 the variable belongs. (Abbreviations - BIP: bipolar disorder; CROSS: cross-disorder; ED: eating  
609 disorder; Drink: drink per week) (b) The loadings of significant nodal brain network measures in the  
610 PGSs-BNMs mode 1. The loading patterns were visualized with R-package 'ggseg' (Mowinckel &  
611 Vidal-Pineiro, 2020) (c) The loadings of significant PGS variables in the PGSs-BNMs mode 2.  
612 (Abbreviations - CP: cognitive performance; EA: educational attainment; DEP: depression; ALCDEP:  
613 alcohol dependence; Smoker: ever smoking) (d) The loadings of significant nodal brain network  
614 measures in the PGSs-BNMs mode 2. (e) The loadings of significant PGS variables in the  
615 phenotypes-BNMs mode 2. The loading patterns of other modes are shown in supplementary figure 6  
616 (abbreviations- NIH: NIH Toolbox score; KSAD: K-SADS (Kiddie Schedule for Affective Disorders and  
617 Schizophrenia; SDS: sleep disturbance scale; CBCL: child behavior checklist; PGBI: parent version of  
618 general behavior inventory) (f) The loadings of significant nodal brain network measures in the  
619 phenotypes-BNMs mode 2.  
620



621

622 **Figure 2 Sparse canonical correlation analysis results of environmental factors-brain network**

623 **measures.** (a) The loadings of environmental variables in mode 2. (b) The loadings of environmental

624 variables in mode 3. Only significant variables are presented. The loadings of corresponding brain

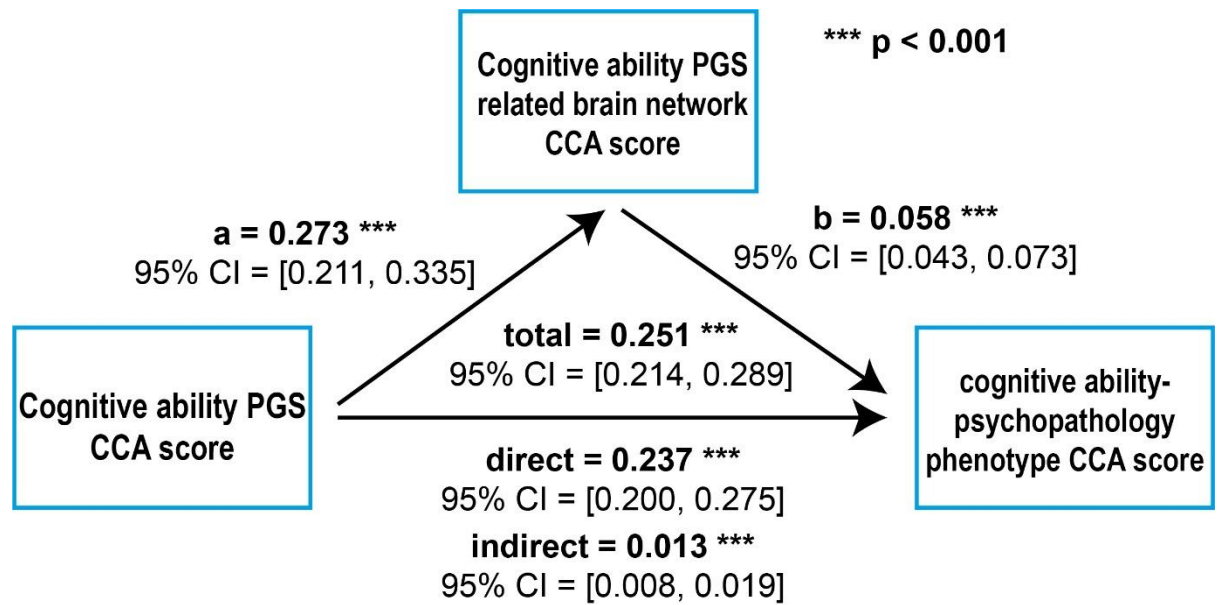
625 network measures are presented in Table 4, and the loading patterns of other modes are shown in

626 supplementary figure 8 (abbreviation – ADI: residential history derived area deprivation index)

627

628

629



631 **Figure 3 Result of mediation analysis.** We used cognitive ability PGS CCA score (i.e., PGS CCA  
632 score of PGS-BNM mode 2) as an independent variable, brain network property CCA score related to  
633 the cognitive ability PGS (i.e., BNM CCA score of PGS-BNM mode 2) as a mediator, and phenotype  
634 of intelligence-psycho pathology CCA score (i.e., phenotype CCA score of Phenotype-BNM mode 2)  
635 as a dependent variable. The p-value and effect size of all paths were presented.

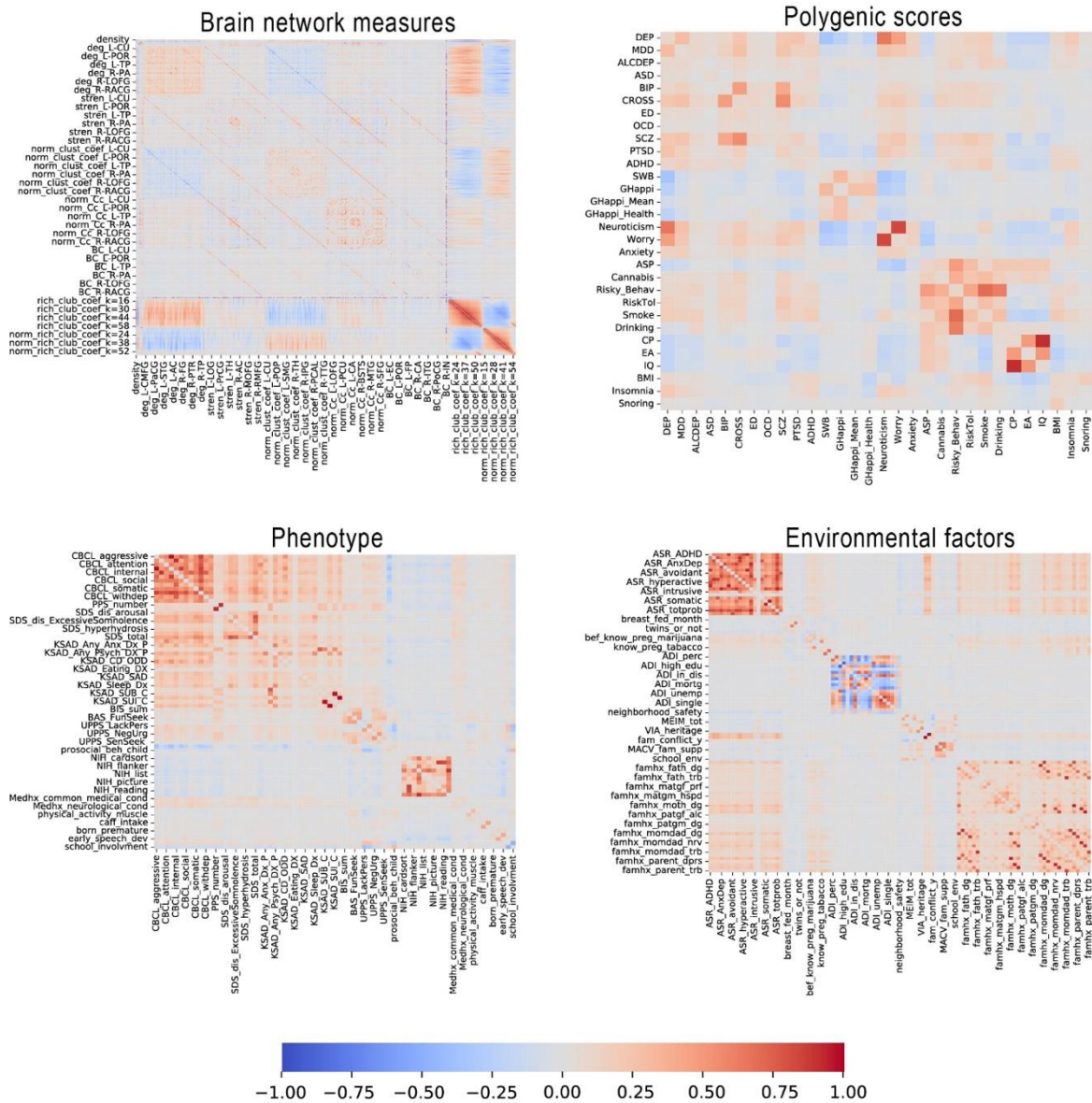
636

637

## 638 **Supplementary Materials**

639

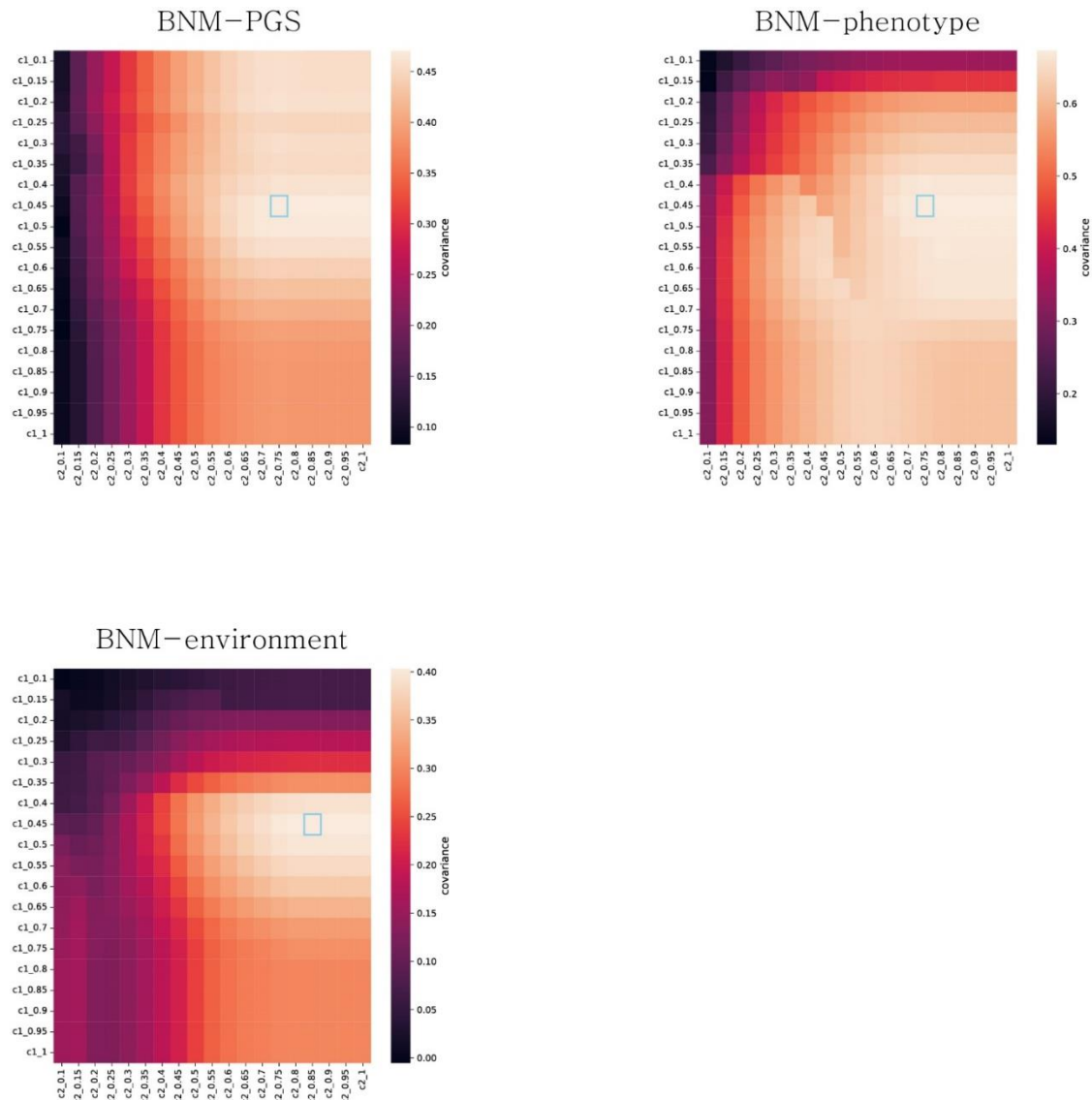




$$\frac{1}{n} X^T X - I$$

640  
641  
642  
643

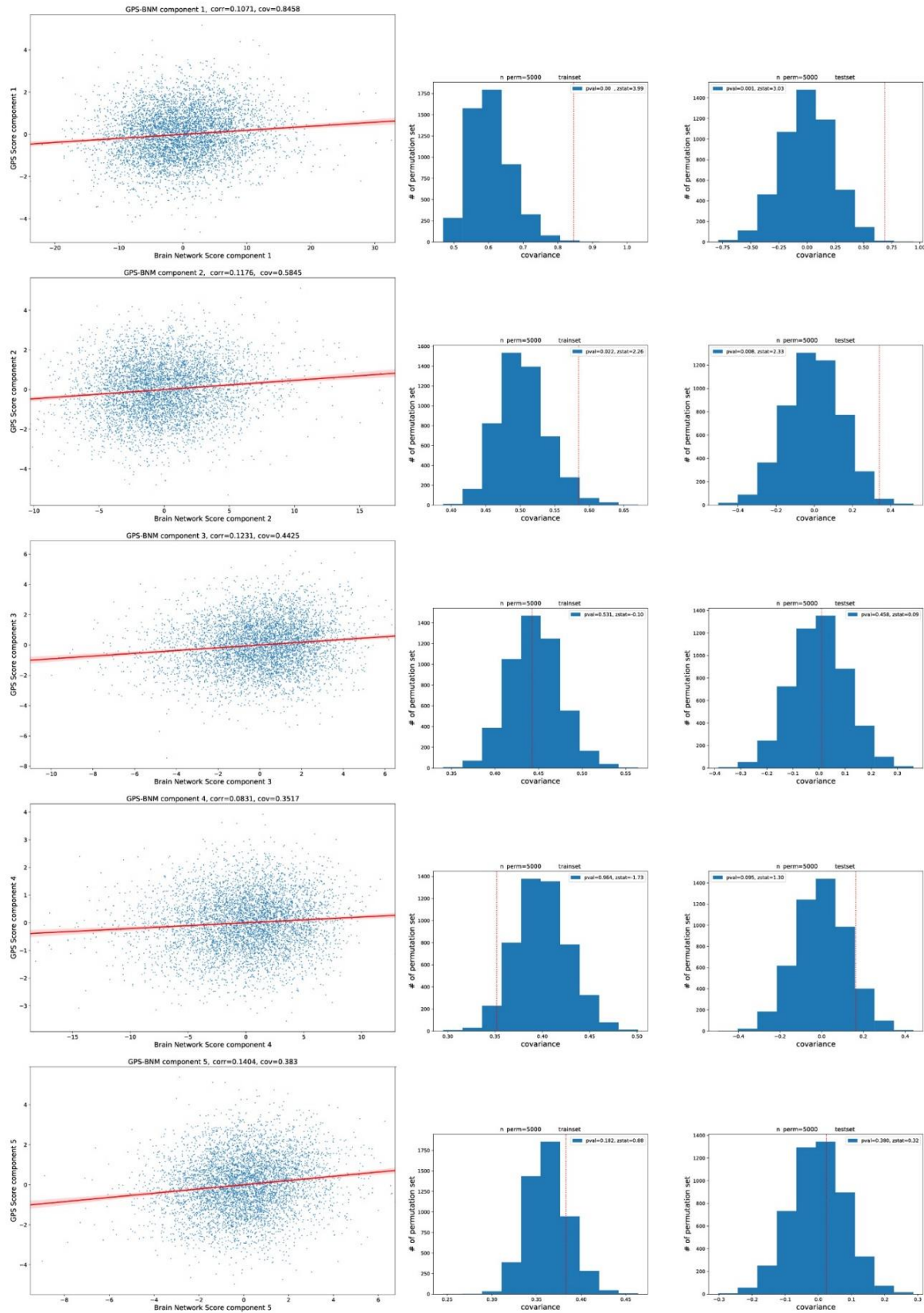
Supplementary Figure 1. Check Witten's assumption.  $\frac{1}{n} X^T X - I$  of the analyzed data is presented. Here, X represents the data from which the variance explained by covariates has been regressed out, as mentioned in the main text.



644

645 **Supplementary Figure 2. Optimal regularization parameters.** We conducted a grid search to  
646 optimize the L1 regularization parameters for Sparse Canonical Correlation Analysis (SCCA). The grid  
647 search ranged from 0.1 to 1 in sparsity parameters, with increments of 0.05. The objective was to  
648 identify the sparsity parameter pair that yielded the highest mean covariance of the first component in  
649 the validation set, using 5-fold cross-validation.

650



651

652 **Supplementary Figure 3. Scatter plots of SCCA scores of brain network measures versus**  
 653 **SCCA scores of polygenic scores and their permutation test results of training and test set.**

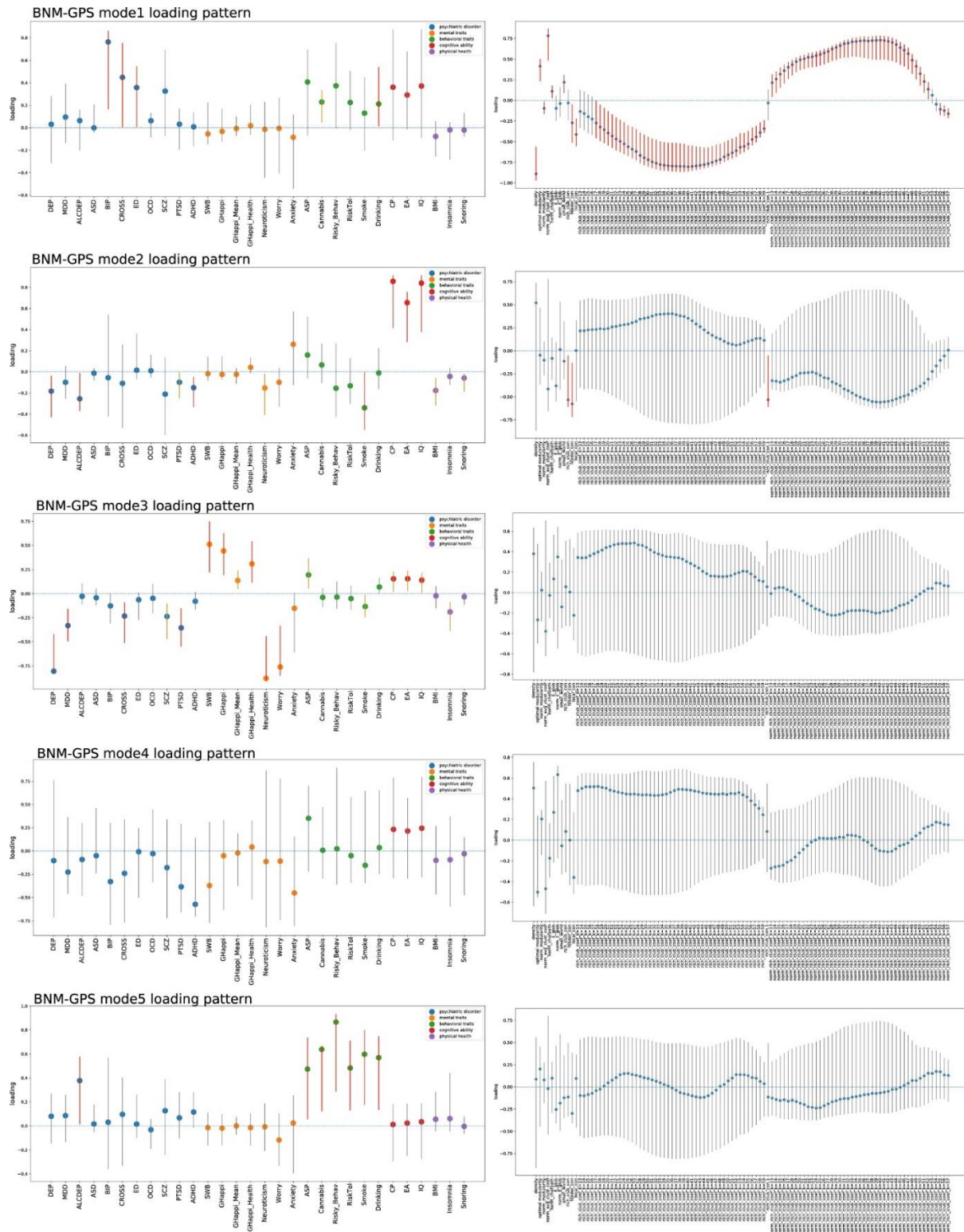
654 Each permutation test result shows the null distribution of SCCA estimated by permutation test.

655 Dashed red line refers to the actual covariance of each mode.

656



657



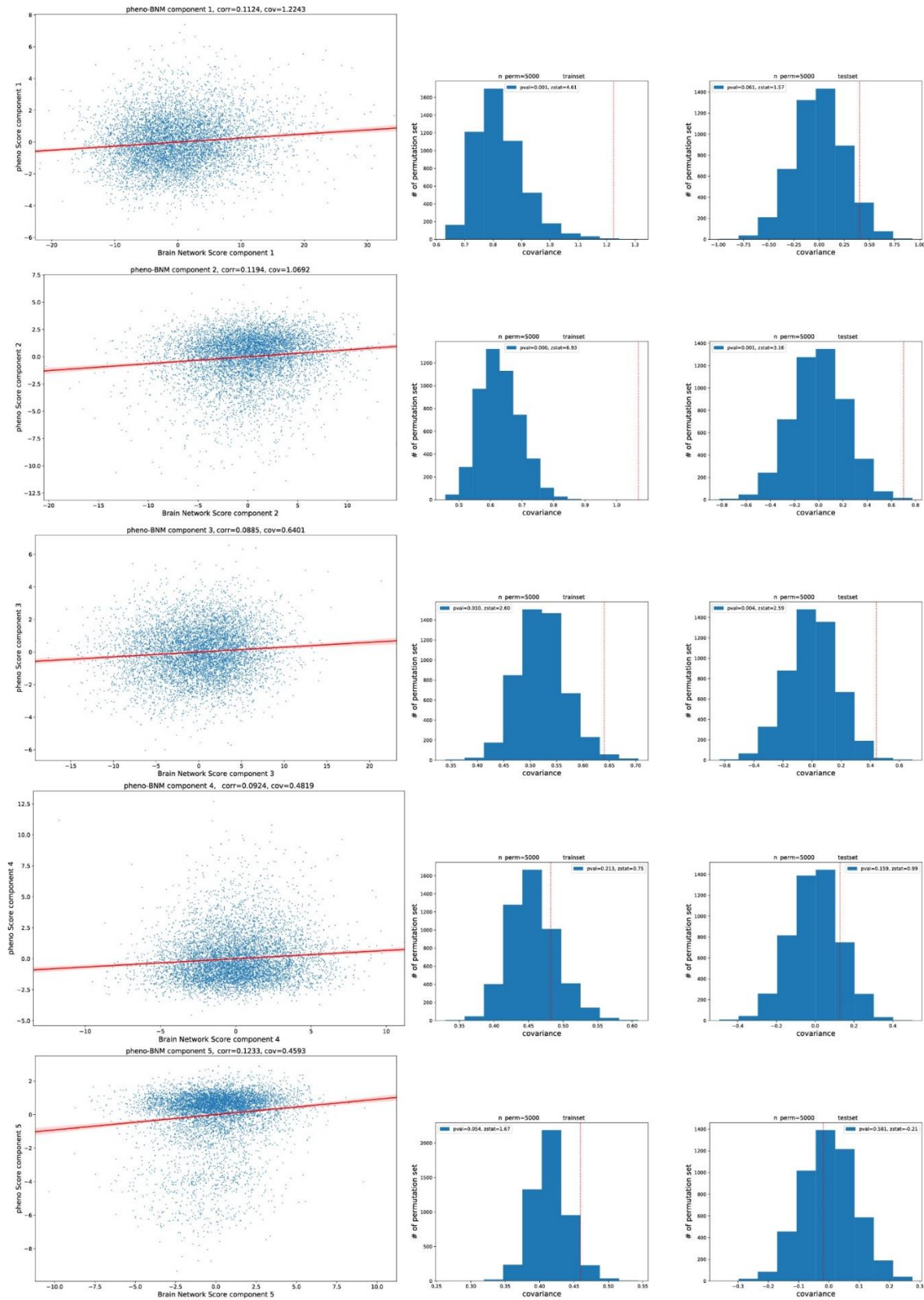
658

659 **Supplementary Figure 4. Sparse CCA loading patterns of brain network measures – polygenic**

660 **scores.** The left column presents the loading of each polygenic score variable, while the right column

661 displays the loadings of global brain network measures and rich club coefficients. Each data point

662 represents the loading value of a specific variable and is color-coded based on its category. The error  
663 bars indicate the 95% confidence interval of the loading, which was estimated using bootstrapping.  
664 Gray-colored error bars indicate a 95% confidence interval that crosses 0. Yellow-colored error bars  
665 indicate a 95% confidence interval that does not cross 0 but corresponds to a variable that is not  
666 frequently selected by Sparse CCA. Red-colored error bars represent a 95% confidence interval that  
667 does not cross 0 and indicates a variable that is frequently selected. Only the variables represented  
668 by red error bars are presented in the main text.



669

670 **Supplementary Figure 5. Scatter plots of SCCA scores of brain network measures versus**

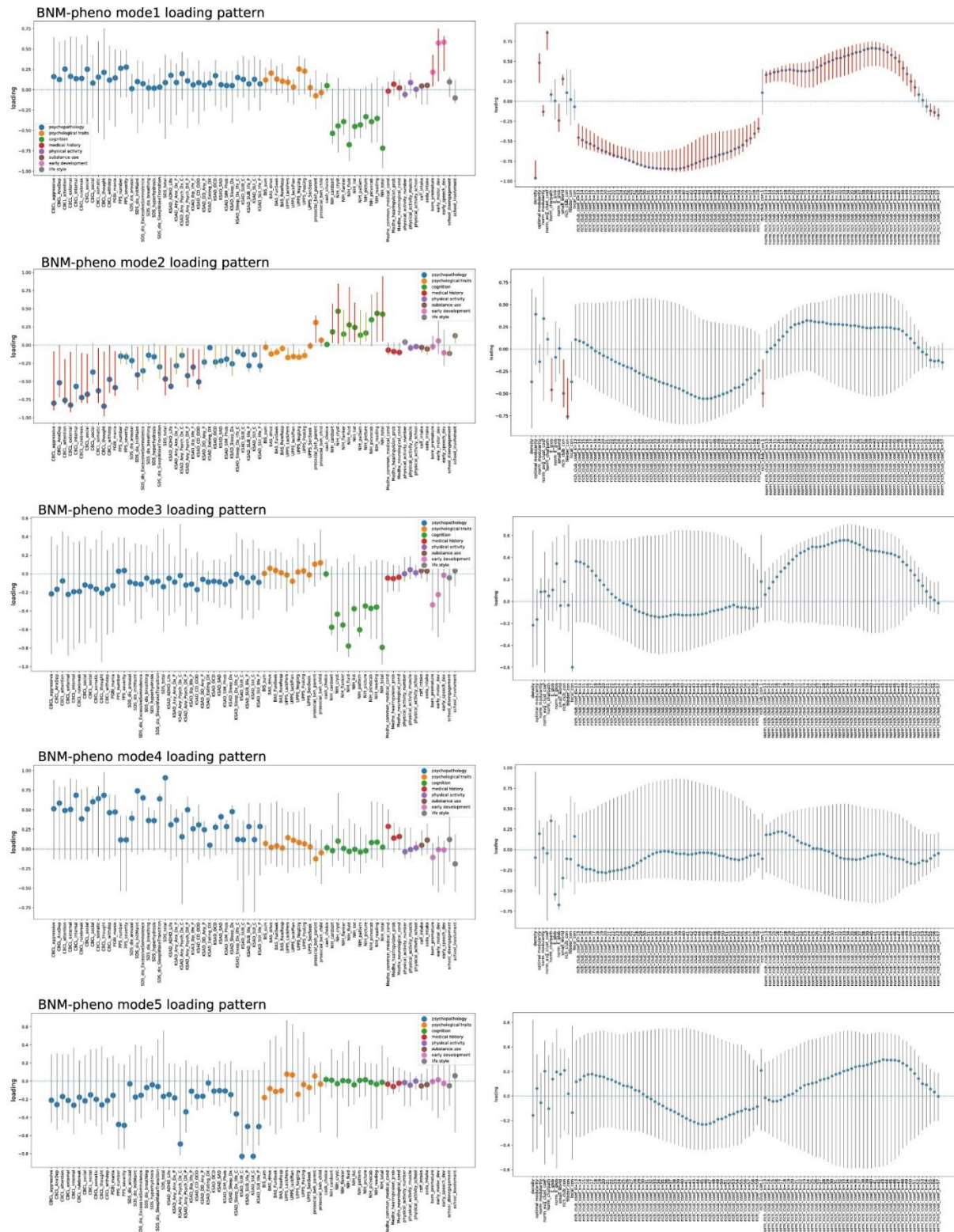
671 **SCCA scores of phenotypic measures and their permutation test results of training and test**

672 **set.** Each permutation test result shows the null distribution of SCCA estimated by permutation test.

673 Dashed red line refers to the actual covariance of each mode.

674





675

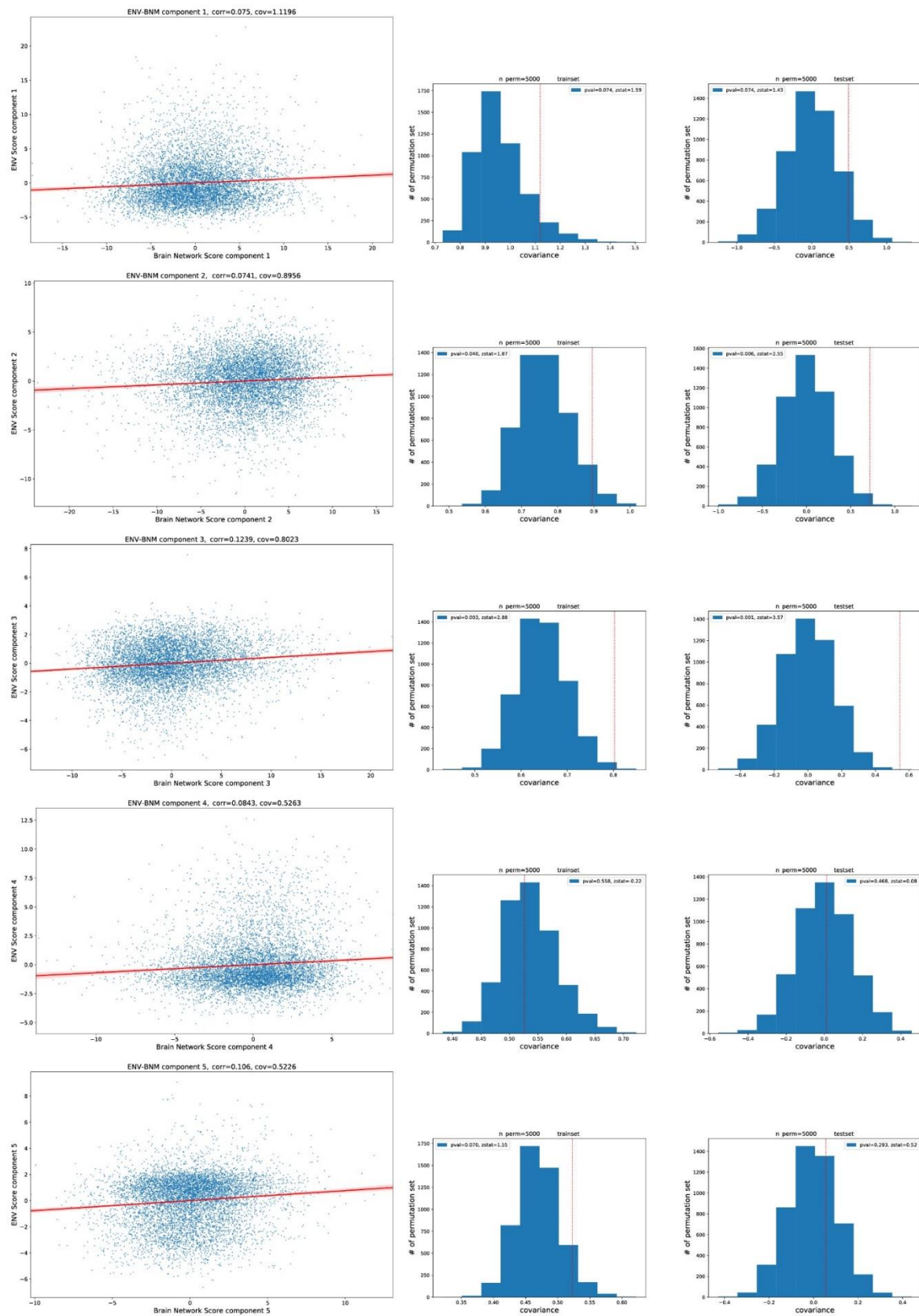
676 **Supplementary Figure 6. Sparse CCA loading patterns of brain network measures – phenotype**

677 **variables.** The left column presents the loading of each phenotype variable, while the right column

678 displays the loadings of global brain network measures and rich club coefficients. Each data point

679 represents the loading value of a specific variable and is color-coded based on its category. The error

680 bars indicate the 95% confidence interval of the loading, which was estimated using bootstrapping.  
681 Gray-colored error bars indicate a 95% confidence interval that crosses 0. Yellow-colored error bars  
682 indicate a 95% confidence interval that does not cross 0 but corresponds to a variable that is not  
683 frequently selected by Sparse CCA. Red-colored error bars represent a 95% confidence interval that  
684 does not cross 0 and indicates a variable that is frequently selected. Only the variables represented  
685 by red error bars are presented in the main text.  
686



687

688 **Supplementary Figure 7. Scatter plots of SCCA scores of brain network measures versus**

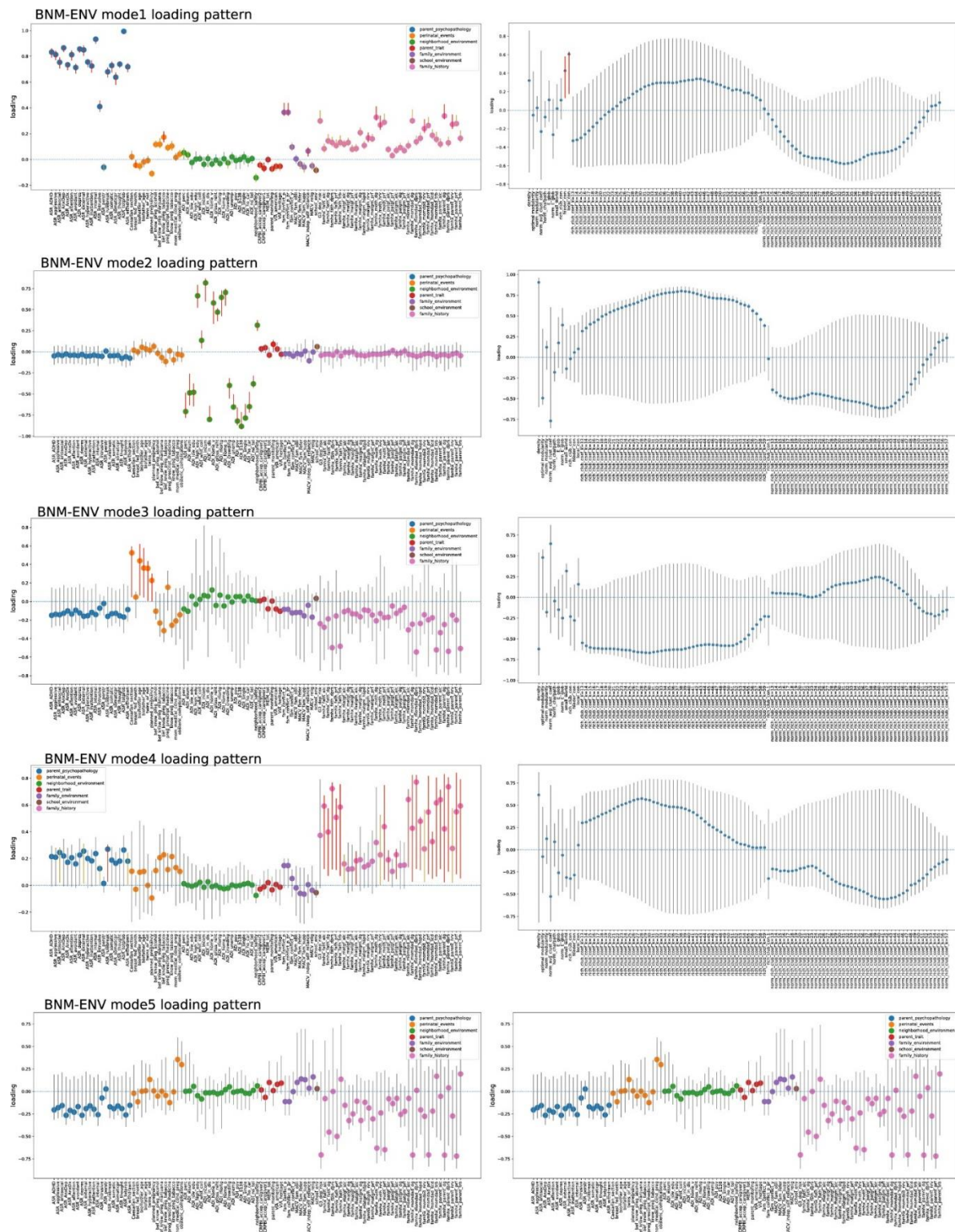
689 **SCCA scores of environmental factors and their permutation test results of training and test**

690 **set.** Each permutation test result shows the null distribution of SCCA estimated by permutation test.

691 Dashed red line refers to the actual covariance of each mode.

692





693

694 **Supplementary Figure 8. Sparse CCA loading patterns of brain network measures –**

695 **environmental factors.** The left column presents the loading of each environmental variable, while

696 the right column displays the loadings of global brain network measures and rich club coefficients.

697 Each data point represents the loading value of a specific variable and is color-coded based on its

698 category. The error bars indicate the 95% confidence interval of the loading, which was estimated  
699 using bootstrapping. Gray-colored error bars indicate a 95% confidence interval that crosses 0.  
700 Yellow-colored error bars indicate a 95% confidence interval that does not cross 0 but corresponds to  
701 a variable that is not frequently selected by Sparse CCA. Red-colored error bars represent a 95%  
702 confidence interval that does not cross 0 and indicates a variable that is frequently selected. Only the  
703 variables represented by red error bars are presented in the main text.

704

## 705 References

706

- 707 Achard, S., & Bullmore, E. (2007). Efficiency and cost of economical brain functional  
708 networks. *PLoS Comput Biol*, 3(2), e17. <https://doi.org/10.1371/journal.pcbi.0030017>
- 709 Akiyama, M., Okada, Y., Kanai, M., Takahashi, A., Momozawa, Y., Ikeda, M., Iwata, N.,  
710 Ikegawa, S., Hirata, M., Matsuda, K., Iwasaki, M., Yamaji, T., Sawada, N., Hachiya,  
711 T., Tanno, K., Shimizu, A., Hozawa, A., Minegishi, N., Tsugane, S., . . . Kamatani, Y.  
712 (2017). Genome-wide association study identifies 112 new loci for body mass index  
713 in the Japanese population. *Nat Genet*, 49(10), 1458-1467.  
714 <https://doi.org/10.1038/ng.3951>
- 715 Alexander-Bloch, A. F., Gogtay, N., Meunier, D., Birn, R., Clasen, L., Lalonde, F., Lenroot, R.,  
716 Giedd, J., & Bullmore, E. T. (2010). Disrupted modularity and local connectivity of  
717 brain functional networks in childhood-onset schizophrenia. *Front Syst Neurosci*, 4,  
718 147. <https://doi.org/10.3389/fnsys.2010.00147>
- 719 Alnaes, D., Kaufmann, T., Marquand, A. F., Smith, S. M., & Westlye, L. T. (2020). Patterns of  
720 sociocognitive stratification and perinatal risk in the child brain. *Proc Natl Acad Sci U*  
721 *S A*, 117(22), 12419-12427. <https://doi.org/10.1073/pnas.2001517117>
- 722 Amare, A. T., Schubert, K. O., Klingler-Hoffmann, M., Cohen-Woods, S., & Baune, B. T.  
723 (2017). The genetic overlap between mood disorders and cardiometabolic diseases:  
724 a systematic review of genome wide and candidate gene studies. *Transl Psychiatry*,  
725 7(1), e1007. <https://doi.org/10.1038/tp.2016.261>
- 726 Athey, S., Tibshirani, J., & Wager, S. (2019). Generalized random forests. *The Annals of*  
727 *Statistics*, 47(2), 1148-1178, 1131. <https://doi.org/10.1214/18-AOS1709>
- 728 Baker, S. T., Lubman, D. I., Yucel, M., Allen, N. B., Whittle, S., Fulcher, B. D., Zalesky, A., &  
729 Fornito, A. (2015). Developmental Changes in Brain Network Hub Connectivity in  
730 Late Adolescence. *J Neurosci*, 35(24), 9078-9087.  
731 <https://doi.org/10.1523/JNEUROSCI.5043-14.2015>
- 732 Barch, D., Pagliaccio, D., Belden, A., Harms, M. P., Gaffrey, M., Sylvester, C. M., Tillman, R.,  
733 & Luby, J. (2016). Effect of Hippocampal and Amygdala Connectivity on the  
734 Relationship Between Preschool Poverty and School-Age Depression. *Am J*  
735 *Psychiatry*, 173(6), 625-634. <https://doi.org/10.1176/appi.ajp.2015.15081014>
- 736 Bassett, D. S., Bullmore, E. T., Meyer-Lindenberg, A., Apud, J. A., Weinberger, D. R., &  
737 Coppola, R. (2009). Cognitive fitness of cost-efficient brain functional networks. *Proc*  
738 *Natl Acad Sci U S A*, 106(28), 11747-11752.  
739 <https://doi.org/10.1073/pnas.0903641106>
- 740 Bathelt, J., Gathercole, S. E., Butterfield, S., team, C., & Astle, D. E. (2018). Children's  
741 academic attainment is linked to the global organization of the white matter  
742 connectome. *Dev Sci*, 21(5), e12662. <https://doi.org/10.1111/desc.12662>
- 743 Bethlehem, R. A. I., Seidlitz, J., White, S. R., Vogel, J. W., Anderson, K. M., Adamson, C.,  
744 Adler, S., Alexopoulos, G. S., Anagnostou, E., Areces-Gonzalez, A., Astle, D. E.,  
745 Auyeung, B., Ayub, M., Bae, J., Ball, G., Baron-Cohen, S., Beare, R., Bedford, S. A.,  
746 Benegal, V., . . . Alexander-Bloch, A. F. (2022). Brain charts for the human lifespan.  
747 *Nature*, 604(7906), 525-533. <https://doi.org/10.1038/s41586-022-04554-y>
- 748 Binder, J. R., Desai, R. H., Graves, W. W., & Conant, L. L. (2009). Where is the semantic  
749 system? A critical review and meta-analysis of 120 functional neuroimaging studies.  
750 *Cereb Cortex*, 19(12), 2767-2796. <https://doi.org/10.1093/cercor/bhp055>
- 751 Bipolar, D., Schizophrenia Working Group of the Psychiatric Genomics Consortium.  
752 Electronic address, d. r. v. e., Bipolar, D., & Schizophrenia Working Group of the

- 753 Psychiatric Genomics, C. (2018). Genomic Dissection of Bipolar Disorder and  
754 Schizophrenia, Including 28 Subphenotypes. *Cell*, 173(7), 1705-1715 e1716.  
755 <https://doi.org/10.1016/j.cell.2018.05.046>
- 756 Bullmore, E., & Sporns, O. (2012). The economy of brain network organization. *Nat Rev*  
757 *Neurosci*, 13(5), 336-349. <https://doi.org/10.1038/nrn3214>
- 758 Bunge, S. A., & Wright, S. B. (2007). Neurodevelopmental changes in working memory and  
759 cognitive control. *Curr Opin Neurobiol*, 17(2), 243-250.  
760 <https://doi.org/10.1016/j.conb.2007.02.005>
- 761 Calamante, F., Tournier, J. D., Jackson, G. D., & Connelly, A. (2010). Track-density imaging  
762 (TDI): super-resolution white matter imaging using whole-brain track-density  
763 mapping. *Neuroimage*, 53(4), 1233-1243.  
764 <https://doi.org/10.1016/j.neuroimage.2010.07.024>
- 765 Chen, T., Chen, Z., & Gong, Q. (2021). White Matter-Based Structural Brain Network of  
766 Major Depression. *Adv Exp Med Biol*, 1305, 35-55. [https://doi.org/10.1007/978-981-33-6044-0\\_3](https://doi.org/10.1007/978-981-33-6044-0_3)
- 768 Clay, H. B., Sullivan, S., & Konradi, C. (2011). Mitochondrial dysfunction and pathology in  
769 bipolar disorder and schizophrenia. *Int J Dev Neurosci*, 29(3), 311-324.  
770 <https://doi.org/10.1016/j.ijdevneu.2010.08.007>
- 771 Collin, G., Scholtens, L. H., Kahn, R. S., Hillegers, M. H. J., & van den Heuvel, M. P. (2017).  
772 Affected Anatomical Rich Club and Structural-Functional Coupling in Young Offspring  
773 of Schizophrenia and Bipolar Disorder Patients. *Biol Psychiatry*, 82(10), 746-755.  
774 <https://doi.org/10.1016/j.biopsych.2017.06.013>
- 775 Conomos, M. P., Miller, M. B., & Thornton, T. A. (2015). Robust inference of population  
776 structure for ancestry prediction and correction of stratification in the presence of  
777 relatedness. *Genet Epidemiol*, 39(4), 276-293. <https://doi.org/10.1002/gepi.21896>
- 778 Conomos, M. P., Reiner, A. P., Weir, B. S., & Thornton, T. A. (2016). Model-free Estimation of  
779 Recent Genetic Relatedness. *Am J Hum Genet*, 98(1), 127-148.  
780 <https://doi.org/10.1016/j.ajhg.2015.11.022>
- 781 Cross-Disorder Group of the Psychiatric Genomics, C. (2013). Identification of risk loci with  
782 shared effects on five major psychiatric disorders: a genome-wide analysis. *Lancet*,  
783 381(9875), 1371-1379. [https://doi.org/10.1016/S0140-6736\(12\)62129-1](https://doi.org/10.1016/S0140-6736(12)62129-1)
- 784 Das, S., Forer, L., Schonherr, S., Sidore, C., Locke, A. E., Kwong, A., Vrieze, S. I., Chew, E.  
785 Y., Levy, S., McGue, M., Schlessinger, D., Stambolian, D., Loh, P. R., Iacono, W. G.,  
786 Swaroop, A., Scott, L. J., Cucca, F., Kronenberg, F., Boehnke, M., . . . Fuchsberger,  
787 C. (2016). Next-generation genotype imputation service and methods. *Nat Genet*,  
788 48(10), 1284-1287. <https://doi.org/10.1038/ng.3656>
- 789 Demontis, D., Walters, R. K., Martin, J., Mattheisen, M., Als, T. D., Agerbo, E., Baldursson,  
790 G., Belliveau, R., Bybjerg-Grauholm, J., Baekvad-Hansen, M., Cerrato, F., Chambert,  
791 K., Churchhouse, C., Dumont, A., Eriksson, N., Gandal, M., Goldstein, J. I., Grasby,  
792 K. L., Grove, J., . . . Neale, B. M. (2019). Discovery of the first genome-wide  
793 significant risk loci for attention deficit/hyperactivity disorder. *Nat Genet*, 51(1), 63-75.  
794 <https://doi.org/10.1038/s41588-018-0269-7>
- 795 Desikan, R. S., Segonne, F., Fischl, B., Quinn, B. T., Dickerson, B. C., Blacker, D., Buckner,  
796 R. L., Dale, A. M., Maguire, R. P., Hyman, B. T., Albert, M. S., & Killiany, R. J. (2006).  
797 An automated labeling system for subdividing the human cerebral cortex on MRI  
798 scans into gyral based regions of interest. *Neuroimage*, 31(3), 968-980.  
799 <https://doi.org/10.1016/j.neuroimage.2006.01.021>
- 800 Fernandez-Cabello, S., Alnaes, D., van der Meer, D., Dahl, A., Holm, M., Kjelkenes, R.,  
801 Maximov, I., Norbom, L. B., Pedersen, M. L., Voldsbekk, I., Andreassen, O. A., &  
802 Westlye, L. T. (2022). Associations between brain imaging and polygenic scores of  
803 mental health and educational attainment in children aged 9-11. *Neuroimage*, 263,  
804 119611. <https://doi.org/10.1016/j.neuroimage.2022.119611>
- 805 Fornito, A., Zalesky, A., & Breakspear, M. (2015). The connectomics of brain disorders. *Nat*  
806 *Rev Neurosci*, 16(3), 159-172. <https://doi.org/10.1038/nrn3901>



- 807 Ge, T., Chen, C. Y., Ni, Y., Feng, Y. A., & Smoller, J. W. (2019). Polygenic prediction via  
808 Bayesian regression and continuous shrinkage priors. *Nat Commun*, *10*(1), 1776.  
809 <https://doi.org/10.1038/s41467-019-09718-5>
- 810 Genomes Project, C., Auton, A., Brooks, L. D., Durbin, R. M., Garrison, E. P., Kang, H. M.,  
811 Korb, J. O., Marchini, J. L., McCarthy, S., McVean, G. A., & Abecasis, G. R. (2015).  
812 A global reference for human genetic variation. *Nature*, *526*(7571), 68-74.  
813 <https://doi.org/10.1038/nature15393>
- 814 Greene, A. S., Shen, X., Noble, S., Horien, C., Hahn, C. A., Arora, J., Tokoglu, F., Spann, M.  
815 N., Carrion, C. I., Barron, D. S., Sanacora, G., Srihari, V. H., Woods, S. W.,  
816 Scheinost, D., & Constable, R. T. (2022). Brain-phenotype models fail for individuals  
817 who defy sample stereotypes. *Nature*, *609*(7925), 109-118.  
818 <https://doi.org/10.1038/s41586-022-05118-w>
- 819 Grove, J., Ripke, S., Als, T. D., Mattheisen, M., Walters, R. K., Won, H., Pallesen, J., Agerbo,  
820 E., Andreassen, O. A., Anney, R., Awashti, S., Belliveau, R., Bettella, F., Buxbaum, J.  
821 D., Bybjerg-Grauholm, J., Baekvad-Hansen, M., Cerrato, F., Chambert, K.,  
822 Christensen, J. H., . . . Borglum, A. D. (2019). Identification of common genetic risk  
823 variants for autism spectrum disorder. *Nat Genet*, *51*(3), 431-444.  
824 <https://doi.org/10.1038/s41588-019-0344-8>
- 825 Hanson, J. L., Chandra, A., Wolfe, B. L., & Pollak, S. D. (2011). Association between income  
826 and the hippocampus. *PLoS One*, *6*(5), e18712.  
827 <https://doi.org/10.1371/journal.pone.0018712>
- 828 Hotelling, H. (1936). Relations between two sets of variates. *Biometrika*, *28*, 321-377.  
829 <https://doi.org/10.1093/biomet/28.3-4.321>
- 830 Howard, D. M., Adams, M. J., Clarke, T. K., Hafferty, J. D., Gibson, J., Shiri, M., Coleman,  
831 J. R. I., Hagenaars, S. P., Ward, J., Wigmore, E. M., Alloza, C., Shen, X., Barbu, M.  
832 C., Xu, E. Y., Whalley, H. C., Marioni, R. E., Porteous, D. J., Davies, G., Deary, I.  
833 J., . . . McIntosh, A. M. (2019). Genome-wide meta-analysis of depression identifies  
834 102 independent variants and highlights the importance of the prefrontal brain  
835 regions. *Nat Neurosci*, *22*(3), 343-352. <https://doi.org/10.1038/s41593-018-0326-7>
- 836 International Obsessive Compulsive Disorder Foundation Genetics, C., & Studies, O. C. D.  
837 C. G. A. (2018). Revealing the complex genetic architecture of obsessive-compulsive  
838 disorder using meta-analysis. *Mol Psychiatry*, *23*(5), 1181-1188.  
839 <https://doi.org/10.1038/mp.2017.154>
- 840 Jansen, P. R., Watanabe, K., Stringer, S., Skene, N., Bryois, J., Hammerschlag, A. R., de  
841 Leeuw, C. A., Benjamins, J. S., Munoz-Manchado, A. B., Nagel, M., Savage, J. E.,  
842 Tiemeier, H., White, T., and Me Research, T., Tung, J. Y., Hinds, D. A., Vacic, V.,  
843 Wang, X., Sullivan, P. F., . . . Posthuma, D. (2019). Genome-wide analysis of  
844 insomnia in 1,331,010 individuals identifies new risk loci and functional pathways.  
845 *Nat Genet*, *51*(3), 394-403. <https://doi.org/10.1038/s41588-018-0333-3>
- 846 Jarrard, L. E. (1993). On the role of the hippocampus in learning and memory in the rat.  
847 *Behav Neural Biol*, *60*(1), 9-26. [https://doi.org/10.1016/0163-1047\(93\)90664-4](https://doi.org/10.1016/0163-1047(93)90664-4)
- 848 Jednorog, K., Altarelli, I., Monzalvo, K., Fluss, J., Dubois, J., Billard, C., Dehaene-Lambertz,  
849 G., & Ramus, F. (2012). The influence of socioeconomic status on children's brain  
850 structure. *PLoS One*, *7*(8), e42486. <https://doi.org/10.1371/journal.pone.0042486>
- 851 Jernigan, T. L., Brown, S. A., & Dowling, G. J. (2018). The Adolescent Brain Cognitive  
852 Development Study. *J Res Adolesc*, *28*(1), 154-156.  
853 <https://doi.org/10.1111/jora.12374>
- 854 Jeurissen, B., Descoteaux, M., Mori, S., & Leemans, A. (2019). Diffusion MRI fiber  
855 tractography of the brain. *NMR Biomed*, *32*(4), e3785.  
856 <https://doi.org/10.1002/nbm.3785>
- 857 Jung, R. E., & Haier, R. J. (2007). The Parieto-Frontal Integration Theory (P-FIT) of  
858 intelligence: converging neuroimaging evidence. *Behav Brain Sci*, *30*(2), 135-154;  
859 discussion 154-187. <https://doi.org/10.1017/S0140525X07001185>
- 860 Karlsson Linner, R., Biroli, P., Kong, E., Meddens, S. F. W., Wedow, R., Fontana, M. A.,

- 861 Lebreton, M., Tino, S. P., Abdellaoui, A., Hammerschlag, A. R., Nivard, M. G., Okbay,  
862 A., Rietveld, C. A., Timshel, P. N., Trzaskowski, M., Vlaming, R., Zund, C. L., Bao, Y.,  
863 Buzdugan, L., . . . Beauchamp, J. P. (2019). Genome-wide association analyses of  
864 risk tolerance and risky behaviors in over 1 million individuals identify hundreds of  
865 loci and shared genetic influences. *Nat Genet*, *51*(2), 245-257.  
866 <https://doi.org/10.1038/s41588-018-0309-3>
- 867 Kim, D. J., Davis, E. P., Sandman, C. A., Glynn, L., Sporns, O., O'Donnell, B. F., & Hetrick,  
868 W. P. (2019). Childhood poverty and the organization of structural brain connectome.  
869 *Neuroimage*, *184*, 409-416. <https://doi.org/10.1016/j.neuroimage.2018.09.041>
- 870 Kim, D. J., Davis, E. P., Sandman, C. A., Sporns, O., O'Donnell, B. F., Buss, C., & Hetrick, W.  
871 P. (2016). Children's intellectual ability is associated with structural network integrity.  
872 *Neuroimage*, *124*(Pt A), 550-556. <https://doi.org/10.1016/j.neuroimage.2015.09.012>
- 873 Kim, K., Joo, Y. Y., Ahn, G., Wang, H. H., Moon, S. Y., Kim, H., Ahn, W. Y., & Cha, J. (2022).  
874 The sexual brain, genes, and cognition: A machine-predicted brain sex score  
875 explains individual differences in cognitive intelligence and genetic influence in young  
876 children. *Hum Brain Mapp*, *43*(12), 3857-3872. <https://doi.org/10.1002/hbm.25888>
- 877 Kim, Y., Vadodaria, K. C., Lenkei, Z., Kato, T., Gage, F. H., Marchetto, M. C., & Santos, R.  
878 (2019). Mitochondria, Metabolism, and Redox Mechanisms in Psychiatric Disorders.  
879 *Antioxid Redox Signal*, *31*(4), 275-317. <https://doi.org/10.1089/ars.2018.7606>
- 880 Koenis, M. M., Brouwer, R. M., van den Heuvel, M. P., Mandl, R. C., van Soelen, I. L., Kahn,  
881 R. S., Boomsma, D. I., & Hulshoff Pol, H. E. (2015). Development of the brain's  
882 structural network efficiency in early adolescence: A longitudinal DTI twin study. *Hum*  
883 *Brain Mapp*, *36*(12), 4938-4953. <https://doi.org/10.1002/hbm.22988>
- 884 Lam, M., Chen, C. Y., Li, Z., Martin, A. R., Bryois, J., Ma, X., Gaspar, H., Ikeda, M.,  
885 Benyamin, B., Brown, B. C., Liu, R., Zhou, W., Guan, L., Kamatani, Y., Kim, S. W.,  
886 Kubo, M., Kusumawardhani, A., Liu, C. M., Ma, H., . . . Huang, H. (2019).  
887 Comparative genetic architectures of schizophrenia in East Asian and European  
888 populations. *Nat Genet*, *51*(12), 1670-1678. [https://doi.org/10.1038/s41588-019-](https://doi.org/10.1038/s41588-019-0512-x)  
889 [0512-x](https://doi.org/10.1038/s41588-019-0512-x)
- 890 Lee, J. J., Wedow, R., Okbay, A., Kong, E., Maghziyan, O., Zacher, M., Nguyen-Viet, T. A.,  
891 Bowers, P., Sidorenko, J., Karlsson Linner, R., Fontana, M. A., Kundu, T., Lee, C., Li,  
892 H., Li, R., Royer, R., Timshel, P. N., Walters, R. K., Willoughby, E. A., . . . Cesarini, D.  
893 (2018). Gene discovery and polygenic prediction from a genome-wide association  
894 study of educational attainment in 1.1 million individuals. *Nat Genet*, *50*(8), 1112-  
895 1121. <https://doi.org/10.1038/s41588-018-0147-3>
- 896 Lett, T., Vogel, B. O., Ripke, S., Wackerhagen, C., Erk, S., Awasthi, S., Trubetskov, V.,  
897 Brandl, E. J., Mohnke, S., Veer, I. M., Nothen, M. M., Rietschel, M., Degenhardt, F.,  
898 Romanczuk-Seiferth, N., Witt, S. H., Banaschewski, T., Bokde, A., Buchel, C.,  
899 Quinlan, E. B., . . . Consortium, I. (2020). Cortical Surfaces Mediate the Relationship  
900 Between Polygenic Scores for Intelligence and General Intelligence. *Cerebral Cortex*,  
901 *30*(4), 2708-2719. <https://doi.org/10.1093/cercor/bhz270>
- 902 Lim, S., Han, C. E., Uhlhaas, P. J., & Kaiser, M. (2015). Preferential detachment during  
903 human brain development: age- and sex-specific structural connectivity in diffusion  
904 tensor imaging (DTI) data. *Cereb Cortex*, *25*(6), 1477-1489.  
905 <https://doi.org/10.1093/cercor/bht333>
- 906 Locke, A. E., Kahali, B., Berndt, S. I., Justice, A. E., Pers, T. H., Day, F. R., Powell, C.,  
907 Vedantam, S., Buchkovich, M. L., Yang, J., Croteau-Chonka, D. C., Esko, T., Fall, T.,  
908 Ferreira, T., Gustafsson, S., Kutalik, Z., Luan, J., Magi, R., Randall, J. C., . . .  
909 Speliotes, E. K. (2015). Genetic studies of body mass index yield new insights for  
910 obesity biology. *Nature*, *518*(7538), 197-206. <https://doi.org/10.1038/nature14177>
- 911 Loh, P. R., Danecek, P., Palamara, P. F., Fuchsberger, C., Y, A. R., H, K. F., Schoenherr, S.,  
912 Forer, L., McCarthy, S., Abecasis, G. R., Durbin, R., & A, L. P. (2016). Reference-  
913 based phasing using the Haplotype Reference Consortium panel. *Nat Genet*, *48*(11),  
914 1443-1448. <https://doi.org/10.1038/ng.3679>

- 915 Luna, B., Padmanabhan, A., & O'Hearn, K. (2010). What has fMRI told us about the  
916 development of cognitive control through adolescence? *Brain Cogn*, 72(1), 101-113.  
917 <https://doi.org/10.1016/j.bandc.2009.08.005>
- 918 Ma, J., Kang, H. J., Kim, J. Y., Jeong, H. S., Im, J. J., Namgung, E., Kim, M. J., Lee, S., Kim,  
919 T. D., Oh, J. K., Chung, Y. A., Lyoo, I. K., Lim, S. M., & Yoon, S. (2017). Network  
920 attributes underlying intellectual giftedness in the developing brain. *Sci Rep*, 7(1),  
921 11321. <https://doi.org/10.1038/s41598-017-11593-3>
- 922 Marek, S., Tervo-Clemmens, B., Calabro, F. J., Montez, D. F., Kay, B. P., Hatoum, A. S.,  
923 Donohue, M. R., Foran, W., Miller, R. L., Hendrickson, T. J., Malone, S. M., Kandala,  
924 S., Feczko, E., Miranda-Dominguez, O., Graham, A. M., Earl, E. A., Perrone, A. J.,  
925 Cordova, M., Doyle, O., . . . Dosenbach, N. U. F. (2022). Reproducible brain-wide  
926 association studies require thousands of individuals. *Nature*, 603(7902), 654-660.  
927 <https://doi.org/10.1038/s41586-022-04492-9>
- 928 Mistic, B., Betzel, R. F., de Reus, M. A., van den Heuvel, M. P., Berman, M. G., McIntosh, A.  
929 R., & Sporns, O. (2016). Network-Level Structure-Function Relationships in Human  
930 Neocortex. *Cereb Cortex*, 26(7), 3285-3296. <https://doi.org/10.1093/cercor/bhw089>
- 931 Modabbernia, A., Janiri, D., Doucet, G. E., Reichenberg, A., & Frangou, S. (2021).  
932 Multivariate Patterns of Brain-Behavior-Environment Associations in the Adolescent  
933 Brain and Cognitive Development Study. *Biol Psychiatry*, 89(5), 510-520.  
934 <https://doi.org/10.1016/j.biopsych.2020.08.014>
- 935 Mowinckel, A. M., & Vidal-Pineiro, D. (2020). Visualization of Brain Statistics With R  
936 Packages ggseg and ggseg3d. *Advances in Methods and Practices in Psychological  
937 Science*, 3(4), 466-483. <https://doi.org/10.1177/2515245920928009>
- 938 Nagel, M., Jansen, P. R., Stringer, S., Watanabe, K., de Leeuw, C. A., Bryois, J., Savage, J.  
939 E., Hammerschlag, A. R., Skene, N. G., Munoz-Manchado, A. B., andMe Research,  
940 T., White, T., Tiemeier, H., Linnarsson, S., Hjerling-Leffler, J., Polderman, T. J. C.,  
941 Sullivan, P. F., van der Sluis, S., & Posthuma, D. (2018). Meta-analysis of genome-  
942 wide association studies for neuroticism in 449,484 individuals identifies novel  
943 genetic loci and pathways. *Nat Genet*, 50(7), 920-927.  
944 <https://doi.org/10.1038/s41588-018-0151-7>
- 945 Namkung, H., Kim, S. H., & Sawa, A. (2017). The Insula: An Underestimated Brain Area in  
946 Clinical Neuroscience, Psychiatry, and Neurology. *Trends Neurosci*, 40(4), 200-207.  
947 <https://doi.org/10.1016/j.tins.2017.02.002>
- 948 Nievergelt, C. M., Maihofer, A. X., Klengel, T., Atkinson, E. G., Chen, C. Y., Choi, K. W.,  
949 Coleman, J. R. I., Dalvie, S., Duncan, L. E., Gelernter, J., Levey, D. F., Logue, M. W.,  
950 Polimanti, R., Provost, A. C., Ratanatharathorn, A., Stein, M. B., Torres, K., Aiello, A.  
951 E., Almli, L. M., . . . Koenen, K. C. (2019). International meta-analysis of PTSD  
952 genome-wide association studies identifies sex- and ancestry-specific genetic risk  
953 loci. *Nat Commun*, 10(1), 4558. <https://doi.org/10.1038/s41467-019-12576-w>
- 954 Okbay, A., Baselmans, B. M., De Neve, J. E., Turley, P., Nivard, M. G., Fontana, M. A.,  
955 Meddens, S. F., Linner, R. K., Rietveld, C. A., Derringer, J., Gratten, J., Lee, J. J., Liu,  
956 J. Z., de Vlaming, R., Ahluwalia, T. S., Buchwald, J., Cavadino, A., Frazier-Wood, A.  
957 C., Furlotte, N. A., . . . Cesarini, D. (2016). Genetic variants associated with  
958 subjective well-being, depressive symptoms, and neuroticism identified through  
959 genome-wide analyses. *Nat Genet*, 48(6), 624-633. <https://doi.org/10.1038/ng.3552>
- 960 Otowa, T., Hek, K., Lee, M., Byrne, E. M., Mirza, S. S., Nivard, M. G., Bigdeli, T., Aggen, S.  
961 H., Adkins, D., Wolen, A., Fanous, A., Keller, M. C., Castelao, E., Kutalik, Z., der  
962 Auwera, S. V., Homuth, G., Nauck, M., Teumer, A., Milaneschi, Y., . . . Hettema, J. M.  
963 (2016). Meta-analysis of genome-wide association studies of anxiety disorders. *Mol  
964 Psychiatry*, 21(10), 1485. <https://doi.org/10.1038/mp.2016.11>
- 965 Pasman, J. A., Verweij, K. J. H., Gerring, Z., Stringer, S., Sanchez-Roige, S., Treur, J. L.,  
966 Abdellaoui, A., Nivard, M. G., Baselmans, B. M. L., Ong, J. S., Ip, H. F., van der Zee,  
967 M. D., Bartels, M., Day, F. R., Fontanillas, P., Elson, S. L., andMe Research, T., de  
968 Wit, H., Davis, L. K., . . . Vink, J. M. (2019). Author Correction: GWAS of lifetime



- 969 cannabis use reveals new risk loci, genetic overlap with psychiatric traits, and a  
970 causal effect of schizophrenia liability. *Nat Neurosci*, 22(7), 1196.  
971 <https://doi.org/10.1038/s41593-019-0402-7>
- 972 Paus, T., Keshavan, M., & Giedd, J. N. (2008). Why do many psychiatric disorders emerge  
973 during adolescence? *Nat Rev Neurosci*, 9(12), 947-957.  
974 <https://doi.org/10.1038/nrn2513>
- 975 Perry, A., Roberts, G., Mitchell, P. B., & Breakspear, M. (2019). Correction: Connectomics of  
976 bipolar disorder: a critical review, and evidence for dynamic instabilities within  
977 interoceptive networks. *Mol Psychiatry*, 24(9), 1398. <https://doi.org/10.1038/s41380-018-0327-7>
- 978
- 979 Phelps, E. A. (2004). Human emotion and memory: interactions of the amygdala and  
980 hippocampal complex. *Curr Opin Neurobiol*, 14(2), 198-202.  
981 <https://doi.org/10.1016/j.conb.2004.03.015>
- 982 Rezin, G. T., Amboni, G., Zugno, A. I., Quevedo, J., & Streck, E. L. (2009). Mitochondrial  
983 dysfunction and psychiatric disorders. *Neurochem Res*, 34(6), 1021-1029.  
984 <https://doi.org/10.1007/s11064-008-9865-8>
- 985 Rodevand, L., Bahrami, S., Frei, O., Chu, Y., Shadrin, A., O'Connell, K. S., Smeland, O. B.,  
986 Elvsashagen, T., Hindley, G. F. L., Djurovic, S., Dale, A. M., Lagerberg, T. V., Steen,  
987 N. E., & Andreassen, O. A. (2021). Extensive bidirectional genetic overlap between  
988 bipolar disorder and cardiovascular disease phenotypes. *Transl Psychiatry*, 11(1),  
989 407. <https://doi.org/10.1038/s41398-021-01527-z>
- 990 Rubin, R. D., Watson, P. D., Duff, M. C., & Cohen, N. J. (2014). The role of the hippocampus  
991 in flexible cognition and social behavior. *Front Hum Neurosci*, 8, 742.  
992 <https://doi.org/10.3389/fnhum.2014.00742>
- 993 Rubinov, M., & Sporns, O. (2010). Complex network measures of brain connectivity: uses  
994 and interpretations. *Neuroimage*, 52(3), 1059-1069.  
995 <https://doi.org/10.1016/j.neuroimage.2009.10.003>
- 996 Rudie, J. D., Brown, J. A., Beck-Pancer, D., Hernandez, L. M., Dennis, E. L., Thompson, P.  
997 M., Bookheimer, S. Y., & Dapretto, M. (2012). Altered functional and structural brain  
998 network organization in autism. *Neuroimage Clin*, 2, 79-94.  
999 <https://doi.org/10.1016/j.nicl.2012.11.006>
- 1000 Savage, J. E., Jansen, P. R., Stringer, S., Watanabe, K., Bryois, J., de Leeuw, C. A., Nagel,  
1001 M., Awasthi, S., Barr, P. B., Coleman, J. R. I., Grasby, K. L., Hammerschlag, A. R.,  
1002 Kaminski, J. A., Karlsson, R., Krapohl, E., Lam, M., Nygaard, M., Reynolds, C. A.,  
1003 Trampush, J. W., . . . Posthuma, D. (2018). Genome-wide association meta-analysis  
1004 in 269,867 individuals identifies new genetic and functional links to intelligence. *Nat*  
1005 *Genet*, 50(7), 912-919. <https://doi.org/10.1038/s41588-018-0152-6>
- 1006 Seghier, M. L. (2013). The angular gyrus: multiple functions and multiple subdivisions.  
1007 *Neuroscientist*, 19(1), 43-61. <https://doi.org/10.1177/1073858412440596>
- 1008 Shao, L., Martin, M. V., Watson, S. J., Schatzberg, A., Akil, H., Myers, R. M., Jones, E. G.,  
1009 Bunney, W. E., & Vawter, M. P. (2008). Mitochondrial involvement in psychiatric  
1010 disorders. *Ann Med*, 40(4), 281-295. <https://doi.org/10.1080/07853890801923753>
- 1011 Shen, H., Gelaye, B., Huang, H., Rondon, M. B., Sanchez, S., & Duncan, L. E. (2020).  
1012 Polygenic prediction and GWAS of depression, PTSD, and suicidal ideation/self-  
1013 harm in a Peruvian cohort. *Neuropsychopharmacology*, 45(10), 1595-1602.  
1014 <https://doi.org/10.1038/s41386-020-0603-5>
- 1015 Smith, R. E., Tournier, J. D., Calamante, F., & Connelly, A. (2013). SIFT: Spherical-  
1016 deconvolution informed filtering of tractograms. *Neuroimage*, 67, 298-312.  
1017 <https://doi.org/10.1016/j.neuroimage.2012.11.049>
- 1018 Smith, S. M., Nichols, T. E., Vidaurre, D., Winkler, A. M., Behrens, T. E., Glasser, M. F.,  
1019 Ugurbil, K., Barch, D. M., Van Essen, D. C., & Miller, K. L. (2015). A positive-negative  
1020 mode of population covariation links brain connectivity, demographics and behavior.  
1021 *Nat Neurosci*, 18(11), 1565-1567. <https://doi.org/10.1038/nn.4125>
- 1022 Sotiropoulos, S. N., & Zalesky, A. (2019). Building connectomes using diffusion MRI: why,

- 1023           how and but. *NMR Biomed*, 32(4), e3752. <https://doi.org/10.1002/nbm.3752>
- 1024   Stahl, E. A., Breen, G., Forstner, A. J., McQuillin, A., Ripke, S., Trubetskov, V., Mattheisen,  
1025   M., Wang, Y., Coleman, J. R. I., Gaspar, H. A., de Leeuw, C. A., Steinberg, S.,  
1026   Pavlidis, J. M. W., Trzaskowski, M., Byrne, E. M., Pers, T. H., Holmans, P. A.,  
1027   Richards, A. L., Abbott, L., . . . Bipolar Disorder Working Group of the Psychiatric  
1028   Genomics, C. (2019). Genome-wide association study identifies 30 loci associated  
1029   with bipolar disorder. *Nat Genet*, 51(5), 793-803. [https://doi.org/10.1038/s41588-019-](https://doi.org/10.1038/s41588-019-0397-8)  
1030   [0397-8](https://doi.org/10.1038/s41588-019-0397-8)
- 1031   Suprano, I., Kocevar, G., Stamile, C., Hannoun, S., Fournier, P., Revol, O., Nusbaum, F., &  
1032   Sappey-Marini, D. (2020). White matter microarchitecture and structural network  
1033   integrity correlate with children intelligence quotient. *Sci Rep*, 10(1), 20722.  
1034   <https://doi.org/10.1038/s41598-020-76528-x>
- 1035   Sweatt, J. D. (2004). Hippocampal function in cognition. *Psychopharmacology (Berl)*, 174(1),  
1036   99-110. <https://doi.org/10.1007/s00213-004-1795-9>
- 1037   Tamnes, C. K., Roalf, D. R., Goddings, A. L., & Lebel, C. (2018). Diffusion MRI of white  
1038   matter microstructure development in childhood and adolescence: Methods,  
1039   challenges and progress. *Dev Cogn Neurosci*, 33, 161-175.  
1040   <https://doi.org/10.1016/j.dcn.2017.12.002>
- 1041   Taquet, M., Smith, S. M., Prohl, A. K., Peters, J. M., Warfield, S. K., Scherrer, B., & Harrison,  
1042   P. J. (2021). A structural brain network of genetic vulnerability to psychiatric illness.  
1043   *Mol Psychiatry*, 26(6), 2089-2100. <https://doi.org/10.1038/s41380-020-0723-7>
- 1044   Tooley, U. A., Mackey, A. P., Ciric, R., Ruparel, K., Moore, T. M., Gur, R. C., Gur, R. E.,  
1045   Satterthwaite, T. D., & Bassett, D. S. (2020). Associations between Neighborhood  
1046   SES and Functional Brain Network Development. *Cereb Cortex*, 30(1), 1-19.  
1047   <https://doi.org/10.1093/cercor/bhz066>
- 1048   Torkamani, A., Wineinger, N. E., & Topol, E. J. (2018). The personal and clinical utility of  
1049   polygenic risk scores. *Nat Rev Genet*, 19(9), 581-590.  
1050   <https://doi.org/10.1038/s41576-018-0018-x>
- 1051   Tournier, J. D., Calamante, F., & Connelly, A. (2007). Robust determination of the fibre  
1052   orientation distribution in diffusion MRI: non-negativity constrained super-resolved  
1053   spherical deconvolution. *Neuroimage*, 35(4), 1459-1472.  
1054   <https://doi.org/10.1016/j.neuroimage.2007.02.016>
- 1055   Tournier, J. D., Smith, R., Raffelt, D., Tabbara, R., Dhollander, T., Pietsch, M., Christiaens,  
1056   D., Jeurissen, B., Yeh, C. H., & Connelly, A. (2019). MRtrix3: A fast, flexible and open  
1057   software framework for medical image processing and visualisation. *Neuroimage*,  
1058   202, 116137. <https://doi.org/10.1016/j.neuroimage.2019.116137>
- 1059   van den Heuvel, M. P., & Fornito, A. (2014). Brain networks in schizophrenia. *Neuropsychol*  
1060   *Rev*, 24(1), 32-48. <https://doi.org/10.1007/s11065-014-9248-7>
- 1061   van den Heuvel, M. P., & Sporns, O. (2011). Rich-club organization of the human  
1062   connectome. *J Neurosci*, 31(44), 15775-15786.  
1063   <https://doi.org/10.1523/JNEUROSCI.3539-11.2011>
- 1064   van den Heuvel, M. P., Sporns, O., Collin, G., Scheewe, T., Mandl, R. C., Cahn, W., Goni, J.,  
1065   Hulshoff Pol, H. E., & Kahn, R. S. (2013). Abnormal rich club organization and  
1066   functional brain dynamics in schizophrenia. *JAMA Psychiatry*, 70(8), 783-792.  
1067   <https://doi.org/10.1001/jamapsychiatry.2013.1328>
- 1068   van den Heuvel, M. P., van Soelen, I. L., Stam, C. J., Kahn, R. S., Boomsma, D. I., &  
1069   Hulshoff Pol, H. E. (2013). Genetic control of functional brain network efficiency in  
1070   children. *Eur Neuropsychopharmacol*, 23(1), 19-23.  
1071   <https://doi.org/10.1016/j.euroneuro.2012.06.007>
- 1072   van Wijk, B. C., Stam, C. J., & Daffertshofer, A. (2010). Comparing brain networks of  
1073   different size and connectivity density using graph theory. *PLoS One*, 5(10), e13701.  
1074   <https://doi.org/10.1371/journal.pone.0013701>
- 1075   Visser, M., Jefferies, E., Embleton, K. V., & Lambon Ralph, M. A. (2012). Both the middle  
1076   temporal gyrus and the ventral anterior temporal area are crucial for multimodal

1077 semantic processing: distortion-corrected fMRI evidence for a double gradient of  
1078 information convergence in the temporal lobes. *J Cogn Neurosci*, 24(8), 1766-1778.  
1079 [https://doi.org/10.1162/jocn\\_a\\_00244](https://doi.org/10.1162/jocn_a_00244)

1080 Walters, R. K., Polimanti, R., Johnson, E. C., McClintick, J. N., Adams, M. J., Adkins, A. E.,  
1081 Aliev, F., Bacanu, S. A., Batzler, A., Bertelsen, S., Biernacka, J. M., Bigdeli, T. B.,  
1082 Chen, L. S., Clarke, T. K., Chou, Y. L., Degenhardt, F., Docherty, A. R., Edwards, A.  
1083 C., Fontanillas, P., . . . Agrawal, A. (2018). Transancestral GWAS of alcohol  
1084 dependence reveals common genetic underpinnings with psychiatric disorders. *Nat*  
1085 *Neurosci*, 21(12), 1656-1669. <https://doi.org/10.1038/s41593-018-0275-1>

1086 Wang, H. T., Smallwood, J., Mourao-Miranda, J., Xia, C. H., Satterthwaite, T. D., Bassett, D.  
1087 S., & Bzdok, D. (2020). Finding the needle in a high-dimensional haystack: Canonical  
1088 correlation analysis for neuroscientists. *Neuroimage*, 216, 116745.  
1089 <https://doi.org/10.1016/j.neuroimage.2020.116745>

1090 Watson, H. J., Yilmaz, Z., Thornton, L. M., Hubel, C., Coleman, J. R. I., Gaspar, H. A.,  
1091 Bryois, J., Hinney, A., Leppa, V. M., Mattheisen, M., Medland, S. E., Ripke, S., Yao,  
1092 S., Giusti-Rodriguez, P., Anorexia Nervosa Genetics, I., Hanscombe, K. B., Purves,  
1093 K. L., Eating Disorders Working Group of the Psychiatric Genomics, C., Adan, R. A.  
1094 H., . . . Bulik, C. M. (2019). Genome-wide association study identifies eight risk loci  
1095 and implicates metabo-psychiatric origins for anorexia nervosa. *Nat Genet*, 51(8),  
1096 1207-1214. <https://doi.org/10.1038/s41588-019-0439-2>

1097 Witten, D. M., Tibshirani, R., & Hastie, T. (2009). A penalized matrix decomposition, with  
1098 applications to sparse principal components and canonical correlation analysis.  
1099 *Biostatistics*, 10(3), 515-534. <https://doi.org/10.1093/biostatistics/kxp008>

1100 Wray, N. R., Ripke, S., Mattheisen, M., Trzaskowski, M., Byrne, E. M., Abdellaoui, A.,  
1101 Adams, M. J., Agerbo, E., Air, T. M., Andlauer, T. M. F., Bacanu, S. A., Baekvad-  
1102 Hansen, M., Beekman, A. F. T., Bigdeli, T. B., Binder, E. B., Blackwood, D. R. H.,  
1103 Bryois, J., Buttenschon, H. N., Bybjerg-Grauholm, J., . . . Major Depressive Disorder  
1104 Working Group of the Psychiatric Genomics, C. (2018). Genome-wide association  
1105 analyses identify 44 risk variants and refine the genetic architecture of major  
1106 depression. *Nat Genet*, 50(5), 668-681. <https://doi.org/10.1038/s41588-018-0090-3>

1107 Xia, C. H., Ma, Z., Ciric, R., Gu, S., Betzel, R. F., Kaczkurkin, A. N., Calkins, M. E., Cook, P.  
1108 A., Garcia de la Garza, A., Vandekar, S. N., Cui, Z., Moore, T. M., Roalf, D. R.,  
1109 Ruparel, K., Wolf, D. H., Davatzikos, C., Gur, R. C., Gur, R. E., Shinohara, R. T., . . .  
1110 Satterthwaite, T. D. (2018). Linked dimensions of psychopathology and connectivity  
1111 in functional brain networks. *Nat Commun*, 9(1), 3003.  
1112 <https://doi.org/10.1038/s41467-018-05317-y>

1113 Xu, L., Skoularidou, M., Cuesta-Infante, A., & Veeramachaneni, K. (2019). Modeling tabular  
1114 data using conditional gan. *Advances in neural information processing systems*, 32.

1115 Zuccoli, G. S., Saia-Cereda, V. M., Nascimento, J. M., & Martins-de-Souza, D. (2017). The  
1116 Energy Metabolism Dysfunction in Psychiatric Disorders Postmortem Brains: Focus  
1117 on Proteomic Evidence. *Front Neurosci*, 11, 493.  
1118 <https://doi.org/10.3389/fnins.2017.00493>